


國立交通大學

電信工程學系

碩士論文

正交分頻多工存取多細胞蜂巢式系統採用各種干擾處理技術之性能評估

The logo of National Tsing Hua University is a circular emblem with a blue border. Inside, there is a stylized figure holding a torch, with the year '1896' at the bottom. The text 'Performance Evaluation of OFDMA Multi-Cellular Systems With Various Interference Management Techniques' is centered below the logo.

Performance Evaluation of OFDMA
Multi-Cellular Systems With Various
Interference Management Techniques

研究生：黃偉賢

指導教授：王蒞君 博士

中華民國九十七年七月

正交分頻多工存取多細胞蜂巢式系統採用各種干擾處理技術之性能評估

Performance Evaluation of OFDMA Multi-Cellular Systems With Various Interference Management Techniques


研究生：黃偉賢

Student：Wei-Hsien Huang

指導教授：王蒞君

Advisor：Li-Chun Wang

國立交通大學
電信工程學系
碩士論文



Performance of Multi-Cell OFDMA Systems
Submitted to Department of Communication Engineering
College of Electrical and Computer Engineering
National Chiao Tung University
in partial Fulfillment of the Requirements
for the Degree of
Master
in
Communication Engineering

July 2008

Hsinchu, Taiwan, Republic of China

中華民國九十七年七月

正交分頻多工存取多細胞蜂巢式系統採用各種干擾處理技術之性能評估

學生：黃偉賢

指導教授：王蒞君

國立交通大學

電信工程學系

摘 要

本論文主要目標在研究以正交分頻多工 (Orthogonal Frequency Division Multiple Access) 蜂巢式網路系統為基礎，配合不同的干擾處理技術，包括：干擾平均 (Interference Averaging)、干擾迴避 (Interference Avoidance) 及干擾消除 (Interference Mitigation) 等技術，討論這些技術對於系統性能的影響。在蜂巢式網路系統中，細胞之間的干擾會嚴重影響系統在的效能。能有效抑制干擾的影響是蜂巢式網路系統的重要問題，因為干擾擴展函數只能適用在分碼多工系統 (Code Division Multiple Access) 而無法適用於正交分頻多工系統。

首先，排列 (permutation) 是一種干擾平均的機制。在 WiMAX 中提出了數種分配子載波 (sub-carrier) 到的子通道 (sub-channel) 的排列方式，而排列方式又可分成分散式及連續式兩種。分散式將子通道內之子載波打散至整個頻帶中，連續式則將子載波以連續方式在頻帶中排列。本論文分散式採用部分使用次通道配置 (Partial Usage of the Sub-Channels)，連續式則採用頻帶自適應編碼 (Band AMC – Band Adaptive Modulation Coding)。其次，對於干擾迴避技術，針對不同的頻率重用系數 (Frequency Reuse Factor) 作分析，可以將細胞間訊號干擾作空間上的隔離。在 WiMAX 中，細胞內可以分隔成內外圈兩個區域，而引入了非整數型的頻率重用係數的想法。最後，在干擾消除技術中，不同的指向性天線將能改變系統的干擾，我們將探討三種不同的指向性天線的影響，包括了鑽石扇區式的寬廣波束型 (Wide Beam Tri-Sector with Diamond-Shaped Sector)、狹窄波束型 (Narrow Beam Tri-Sector) 以及五邊形扇區式的寬廣波束型 (Wide Beam Tri-Sector with Pentagon-Shaped Sector) 方向性天線。本論文也採用全向性天線，搭配全部使用通道配置

(Full Usage Sub-Channel)，以比較之間的差異。

在本論文中，模擬的顯示出一些正交分頻多工存取多細胞蜂巢式系統的重要特性：

1. 在時變的無線通道中，採取分散式的排列方式會較有利於系統容量。
2. 頻率重用雖然對於連線品質和系統公平性有些益處，但對於系統的總容量都是沒有幫助的。
3. 而針對於外圈的使用者而言，在重用係數在 2 左右時可以得到容量上的改善。
4. 針對三種指向性天線而言，本論文並不推薦使用 WiMAX 建議的模型（五邊形式的寬廣波束型），改採用狹窄波束型方向性天線能得到較佳的性能。



Summary

The main goal of this thesis is to investigate the performance of orthogonal frequency division multiple access (OFDMA) multi-cellular systems with interference averaging, avoidance, and mitigation techniques. In multi-cellular systems, the inter-cell interference degrades the system performance significantly. Suppressing the interference is an important issue in OFDMA multi-cellular systems because the interference spreading function is only suitable for code division multiple access (CDMA) systems but not for OFDMA systems.

First, permutation belongs to the interference averaging technique. Several permutation methods are proposed to assign sub-carriers in a sub-channel in WiMAX. In the distributed type, the sub-carriers in a sub-channel is randomly distributed in the entire usable frequency band. In the contiguous type, the sub-carriers in a sub-channel is arranged continuously. In this thesis, we call Partial Usage of the Sub-Channels (PUSC)/ Band Adaptive Modulation and Coding (Band AMC) permutation as randomly distributed/contiguous types. Secondly, for the interference avoidance technique, we focus on the frequency reuse technique. WiMAX introduce the structure of inner circle and outer ring in a cell. Thus, the reuse factor can be an integer or a fractional number. Thirdly, for the interference mitigation technique, directional antenna can change the distribution of the interference in the space. We study three different types of antenna patterns: 1) Wide Beam Tri-Sector (WBTC) with Diamond-Shaped Sector; 2) NBTC (Narrow Beam Tri-Sector); 3) WBTC with Pentagon-Shaped Sector. We will also use the Full Usage of Sub-Channels (FUSC) permutation in omnidirectional antenna pattern for comparison.

The simulation results show some important points about the effectiveness of various interference management techniques in OFDMA multi-cellular systems:

1. In a time-varying wireless channel, the randomly distributed permutation approach is better than the contiguous sub-carrier method.

2. Frequency reuse with a higher reuse factor can improve the link quality and system fairness, but decrease capacity.
3. The throughput of the outer ring users may be improved when reuse factor is about two.
4. The antenna pattern suggested by the WiMAX standard, i.e. the WBTC with Pentagon-Shaped Sector, performs worse than NBTC.



Acknowledgments

I would like to thank Dr. Li-Chun Wang who gives me many valuable suggestions in the research. Without his advice and comments, this thesis would not have been finished.

In addition, I am deeply grateful to my laboratory mates Jane-Hwa, Anderson Chen, Hyper, Wei-Cheng, Chu-Jung, Vincent, How-Chen, Chiao, Chiao-Jung, How-Hsiao Lu, and Samer in Wireless System Laboratory. They provide me tons of assistance about my research.



Contents

Summary	v
Acknowledgements	vii
List of Tables	xii
List of Figures	xiii
1 Introduction	1
1.1 History and Development of OFDM/OFDMA	1
1.2 Milestones of IEEE 802.16	1
1.3 Interference in OFDMA Multi-Cellular System	3
1.4 Thesis Outline	3
2 Background	4
2.1 WiMAX in IEEE Wireless Network Families	4
2.2 Downlink/Uplink in WiMAX	5
2.2.1 Downlink (DL)	5
2.2.2 Uplink (UL)	5
2.3 OFDMA in IEEE 802.16	6
2.3.1 PHY Modes	6
2.3.2 OFDMA Air Interface and Frame Structure	6
2.4 OFDMA in LTE	7

3	Simulation Platform	9
3.1	Simulation Assumptions	9
3.2	Path Loss Model	9
3.3	Shadowing Model	12
3.4	Frequency Selective Fading Channel	14
3.5	Thermal Noise Budget	16
3.6	Wrap Around Scheme	16
3.7	Directional Antenna Pattern	17
3.8	Computation of per Sub-channel Effective SINR	18
3.9	Capacity Evaluation	18
3.10	Fairness Index	20
4	Effects of the Interference Averaging Technique: Sub-carrier Per-	
	mutation	21
4.1	Types of Sub-carrier Permutation	21
4.2	Down Link PUSC	22
4.2.1	Symbol Structure	22
4.2.2	Renumbering and Permutation Base Assignment	23
4.2.3	Results of Locations of Sub-carriers in PUSC	25
4.3	Down Link FUSC Permutation	27
4.4	Down Link Band AMC Permutation	27
4.5	Numerical Results	29
4.5.1	Comparison of PUSC and Band AMC	30
4.5.2	Comparison of Distributed or Contiguous Sub-Carriers	31
5	Effects of the Interference Avoidance Technique: Frequency Reuse	32
5.1	Types of Frequency Reuse	32
5.1.1	Regular Frequency Reuse	32
5.1.2	Fractional Frequency Reuse	34

5.1.3	Achievable FFR Factors	35
5.2	Inner Circle and Outer Ring User Decision	35
5.3	Permutation Base Assignment in Frequency Reuse	38
5.4	Relation of Frequency Reuse and Throughput	39
5.5	Numerical Results	40
5.5.1	Effects of FFR on SINR	40
5.5.2	Effects of FFR on Link Quality	40
5.5.3	Effects of FFR on Throughput	43
5.5.4	Effects of FFR on Inner Circle and Outer Ring Users	43
5.5.5	Comparison of PUSC Type 0 and 1	45
6	Effects of the Interference Mitigation Technique: Directional Antenna	47
6.1	Types of Directional Antenna	47
6.1.1	WBTC with Diamond-Shaped Sector	50
6.1.2	NBTC	51
6.1.3	WBTC with Pentagon-Shaped Sector	52
6.2	Omnidirectional Antenna and FUSC	53
6.3	Numerical Results	54
6.3.1	Effect on Throughput	54
6.3.2	Effect on Link Quality	55
6.3.3	Effect on the Capacity and Fairness of Inner/Outer Users	56
7	Conclusion and Future Work	62
7.1	Conclusion	62
7.1.1	Permutation	62
7.1.2	Regular/Fractional Frequency Reuse	63
7.1.3	Directional Antenna	63
7.2	Future Work	64

7.2.1	Benefit of Band AMC	64
7.2.2	Proportional Fair Scheduling	64
	Bibliography	66
	Vita	68



List of Tables

1.1	IEEE 802.16 Development	2
3.1	Simulation Assumptions	10
3.2	Path Loss Parameters in Different Types of Terrains	11
3.3	Types of Terrains	12
3.4	PHY Parameters in This Thesis and in [8]	19
4.1	Permutation Types in WiMAX	22
4.2	PUSC Sub-Channels	24
4.3	Permutation Base	25
4.4	Band AMC Sub-Channels	28
4.5	The 90% Tile of Users' Received SINR for Fig. 4.8	30
5.1	FFR Values	36
5.2	Permutation Base Assignment with Frequency Reuse	39
6.1	The Three Directional Antennas	47

List of Figures

2.1	IEEE Wireless Networks	4
2.2	A WiMAX OFDMA Symbol Sample	7
2.3	LTE OFDMA Downlink Resource Assignment in Time and Frequency	8
3.1	Effect of Distance on Path Loss in the Terrain Type A of Propagation Model of IEEE 802.16 WiMAX	13
3.2	Time Domain Response of Stanford University Interim Channel Model (SUI)	14
3.3	Frequency Domain Response of SUI-3 Model	15
3.4	The 19 Cells in the Multi-Cellular System	17
3.5	Effect of Various SINR on the Throughput with Different Modulation and Coding Schemes	19
4.1	PUSC Symbol Structure	23
4.2	PUSC Cluster Structure	23
4.3	PUSC Sub-Channel Generation	25
4.4	Sub-Carriers of Different Sub-Channels when $DL_PermBase = 0$	26
4.5	Sub-Carriers in the 7th Sub-Channel for Various Value of $DL_PermBase$	26
4.6	FUSC Symbol structure and Sub-Channel Generation	27
4.7	Band AMC Bin and Sub-Channel Structure	28
4.8	The Users' SINR in PUSC Type 0, PUSC Type 1, and Band AMC	29
4.9	The 90% Tile of Users' Received SINR Figure	30

4.10	Comparison of Randomly Distributed and Contiguous Subcarrier Permutations	31
5.1	Cell Planning when Reuse Factor $N= 3, 4,$ and 7	33
5.2	Fractional Frequency Reuse	34
5.3	Signal Strength in a 2G System Cell Phone	37
5.4	Selection of Inner and Outer Users by Sorting on Received Power Strengths	37
5.5	Interference Sources of Different Permutation Base Assignment in Reuse Factor $N= 3$	38
5.6	Trends of Reuse Factor and Throughput (\uparrow <i>Increasing</i> , \downarrow <i>Decreasing</i>)	40
5.7	CDF of SINR in PUSC Type 0 and Type 1, Band AMC with Varies Reuse Factor in Interference Traffic Load= 100%	41
5.8	CDF of SINR in FUSC Type 0 and Type 1 with Varies Reuse Factor in Interference Traffic Load= 100%	42
5.9	The 90% Tile of Users' Received SINR v.s. Reuse Factor	42
5.10	Reuse Factor and Cell Capacity	43
5.11	The Cell Capacity of Inner/Outer Users in PUSC Type 1	44
5.12	The Fairness Index of the Users' Throughput in PUSC Type 1	45
5.13	The Path Loss of Interference Sources from Different Users A, B, and C	46
6.1	Antenna Gain	48
6.2	The Three Antenna Patterns in Multi-Cellular Environment	49
6.3	WBTC with Diamond-Shaped Sector Antenna Pattern and Cell Boundary	50
6.4	NBTC Antenna Pattern and Cell Boundary	51
6.5	WBTC with Pentagon-Shaped Sector Antenna Pattern and Cell Boundary	52
6.6	The Sub-Channels and Pilots in FUSC Permutation	53

6.7 Omnidirectional Antenna Pattern and Cell Boundary	53
6.8 Cell Capacity in Three Different Directional Antennas	54
6.9 Cell Capacity in Directional and Omnidirectional Antennas	55
6.10 The 90% tile of Users' Received SINR in Different Antennas	56
6.11 Inner Users' Throughput in Three Different Directional Antennas . .	57
6.12 Outer Users' Throughput in Three Different Directional Antennas . .	58
6.13 Inner Users' Throughput in Directional and Omnidirectional Antennas	59
6.14 Outer Users' Throughput in Directional and Omnidirectional Antennas	60
6.15 The Fairness of the Users in Directional and Omnidirectional Antenna Systems	61



CHAPTER 1

Introduction

1.1 History and Development of OFDM/OFDMA

Orthogonal frequency division multiplexing (OFDM) is an important modulation communication method. Furthermore, orthogonal frequency division multiple access (OFDMA) is a multi-channel version of OFDM by grouping the sub-carriers into some sub-channels. Multiple users can access the network simultaneously in different sub-channels.

The key concept of OFDM is to apply the fast fourier transformation (FFT) in multi-carrier communications. Although the algorithm is too complicated to implement 40 years ago, the recent development of FFT has greatly reduced the difficulty of using OFDM in real communication systems. In 1985, Cimini [4] suggested using OFDM for mobile communications. Nowadays, the OFDM and OFDMA methods have been used in several systems such as DVB-T, IEEE 802.11a/g, 3GPP Long Term Evolution (LTE), IEEE 802.22 , and WiMAX etc.

1.2 Milestones of IEEE 802.16

IEEE 802.16 Worldwide Interoperability for Microwave Access (WiMAX) is the Standard for wireless metropolitan area networks. The major milestones of IEEE 802.16

are shown in Table 1.1.

Table 1.1: IEEE 802.16 Development

Year	Version	Spectrum	Comment
2001	802.16	10-66GHz	Fixed Stations
2003	802.16a	2-11 GHz	Fixed Stations
2004	802.16d	2-66 GHz	Fixed Stations
2005	802.16e	2- 6 GHz	Mobile Stations Included
2007	802.16j	10-66 GHz	Relay Stations Included
2008	802.16m	2- 6 GHz	Next Generation of 802.16e

The concept of the IEEE 802.16 WiMAX was started in 1999. The success of wireless local area network (WLAN) inspired the communication engineers to seek a network for larger area applications. In the beginning, the IEEE 802.16 is designed with single carrier transmission. However, the OFDM/OFDMA modes are introduced in IEEE 802.16a/d. Then, the mobility issues are considered in the IEEE 802.16e WiMAX, and more modes are proposed such as different FFT sizes and permutation types.

The IEEE 802.16j WiMAX defines the usage of relay stations in the WiMAX. In the metropolitan area, the system coverage and capacity are limited by the severe fading and shadowing. Spreading the relay stations in the cell can avoid poor transition paths and improve signal strength.

The IEEE 802.16m WiMAX, or called the next generation of the 802.16e WiMAX, is designed to achieve the objectives of the International Mobile Telecommunications (IMT-Advanced System) [5], i.e. 4 G system. The data rates are 100 Mbps or 1 Gbps in high or low speed mobility conditions.

1.3 Interference in OFDMA Multi-Cellular System

Interference is a severe problem in OFDMA multi-cellular systems. The signals of sub-carriers in OFDMA are orthogonal to each other without frequency offset. Thus, the users with different sub-channels will not suffer from the interference generating by the other users in the same cell. However, the co-channel interference from the adjacent cells is still a severe problem. The three main methods to overcome the interference are: 1) interference averaging [1]; 2) interference avoidance [2]; 3) interference mitigation [3]. In this thesis, we will perform simulations to investigate the interference issues in the IEEE 802.16 WiMAX. We study permutation algorithm, fractional frequency reuse technology, and the directional antennas.

1.4 Thesis Outline

The rest of this thesis are organized as follows. Chapter 2 introduces OFDMA in WiMAX and LTE systems. Chapter 3 introduces the simulation platform developed in this thesis. Chapter 4 introduces the interference averaging techniques, i.e. permutation methods. Chapter 5 introduces the interference avoidances techniques, i.e. frequency reuse methods. Chapter 6 introduces the interference mitigation techniques, i.e. directional antenna methods. Chapter 7 gives the conclusion and suggestion for the future works.

CHAPTER 2

Background

2.1 WiMAX in IEEE Wireless Network Families

There are many IEEE standards for various wireless networks. In Fig. 2.1, Bluetooth, WiFi, WiMAX, and IEEE 802.22 are important members of this family for different applications. In this thesis, we focus on the performance evaluation of WiMAX. WiMAX is designed for the metropolitan area services. The separation distance between base stations in WiMAX ranges in several kilo-meters.

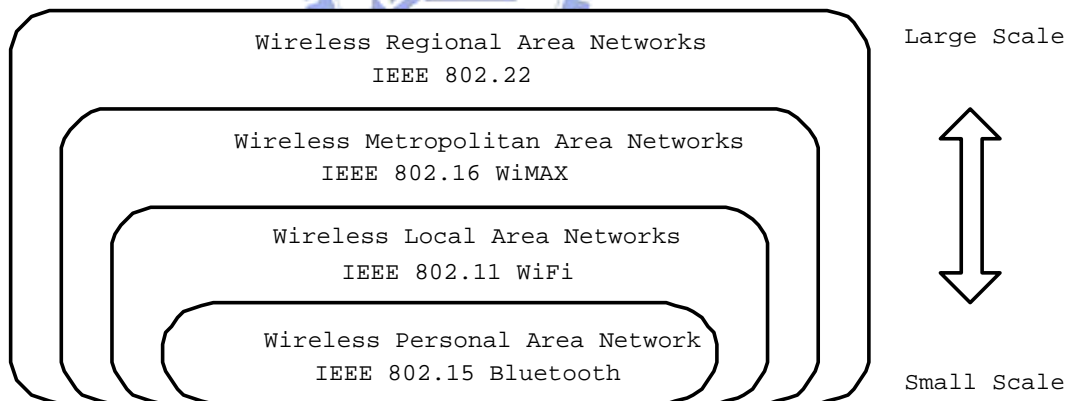


Figure 2.1: IEEE Wireless Networks

Initially, WiMAX adopts the OFDM in the PHY layer. The bandwidth efficiency of OFDM is better than legacy FDM. With cyclic prefix, OFDM can overcome the multi-path fading. The time domain equalizers in the GSM and CDMA systems

are more complicated than OFDM. Hence, WiMAX is a promising solution to the last mile problem.

2.2 Downlink/Uplink in WiMAX

2.2.1 Downlink (DL)

WiMAX is an infrastructure-based network. There is a base station (BS) in a cell. The BS will broadcast preambles periodically to the mobile stations (MS). The preambles will help the MSs in BS recognition, frame detection, and signal synchronization. Frame control header (FCH) is next to the preamble and coding with predefined modulation coding scheme. MSs will read the FCH and get the information about this frame. The information includes: the DL/UL map, DL/UL channel descriptors, et, al. MSs can read the DL data according to the instructions in DL map.

2.2.2 Uplink (UL)

The UL part in a frame is followed behind the Time Transition Gap (TTG). Different MSs will have different TTGs in order to solve the near-far problem. Sending data to BS simultaneously by different MSs in different locations is achievable in OFDMA mode. MS must read and decode the UL map and send the data in the correct time and sub-channel which are assigned by BS. Different sub-channels will not share the same pilots in order to avoid the intra-cell interference.

2.3 OFDMA in IEEE 802.16

2.3.1 PHY Modes

IEEE 802.16 WiMAX supports four PHY modes. Single carrier is the original mode. The OFDM and OFDMA modes are usually used in recent applications. TDM can be applied in OFDM when the system need multiplexing. Hybrid of TDM and FDM can result in four OFDMA modes:

- 1) single carrier in 10-66 GHz;
- 2) single carrier a in sub-11 GHz with frequency domain equalization;
- 3) OFDM in sub-11 GHz with fixed FFT size (256);
- 4) OFDMA in sub-11 GHz with scalable FFT size (128, 512, 1024, and 2048).

2.3.2 OFDMA Air Interface and Frame Structure

In the OFDM mode, the data is transmitted by many orthogonal sub-carriers. The major merits of OFDMA include high efficiency of spectrum usage, simpler frequency domain equalizer, and resistance against the multi-path fading. Pilot tones are distributed among the data carriers in order to estimate the channel. An overhead which called cyclic prefix (CP) is added in every OFDM symbol for synchronization to overcome the multi-path fading. The OFDMA is an extension version of OFDM, where sub-carriers are divided into groups, called sub-channels. Stations can use hybrid of FDM and TDM multiplexing.

The frame structure in OFDMA is shown in Fig. 2.2. An OFDMA symbol consists preamble, FCH, DL, and UL parts. The TTG is placed between DL and UL parts. It's used for solving the near-far problem.

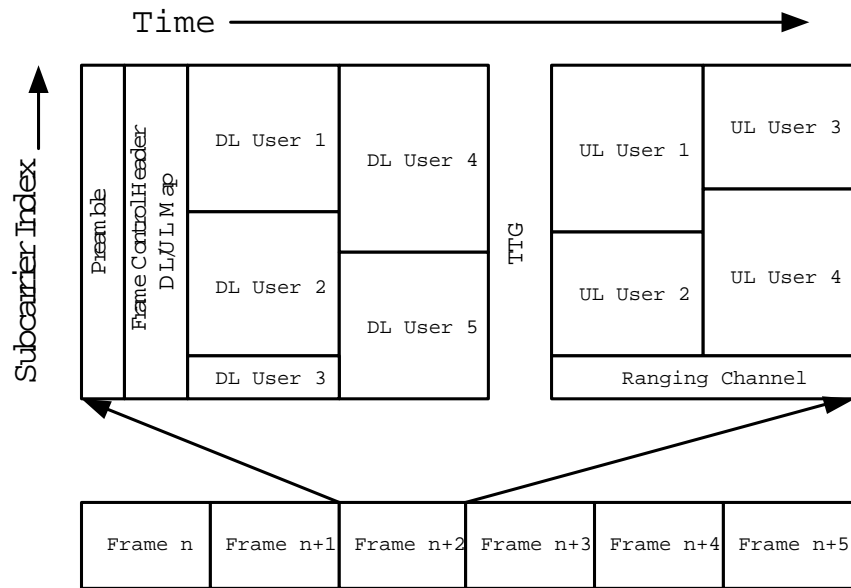


Figure 2.2: A WiMAX OFDMA Symbol Sample

2.4 OFDMA in LTE

Long term evolution (LTE) standard in the third generation partnership project (3GPP) is targeted on the market in the next ten years. The communication vendors may deploy the 4G networks using LTE technology as a foundation. LTE is a strong competitor for WiMAX. The goals of the uplink and downlink throughput of LTE are 50, 100 Mbps, respectively.

The OFDMA method will be applied for the physical-layer downlink transmission technique in the LTE system. The 3G systems use the CDMA modulation, but CDMA is not very suitable for the MIMO-based signal processing. OFDMA is a good modulation for MIMO signal processing. However, because of the severe peak to average power ratio (PAPR) problem, the FDMA is used instead of OFDMA in the uplink transmission for LTE. Another merit of FDMA is the power consumption is less than OFDMA. Power consumption is a severe problem for MSs. The minimum

resource block consists of 14 symbols and 12 sub-carriers. A sample of LTE OFDMA DL assignment is shown as Fig. 2.3.

Frequency	User1	User2	User2	User3	User3
	User1	User2	User2	User4	User3
	User4	User2	User4	User4	User1
	User4	User1	User3	User1	User1
	User4	User1	User3	User1	User1
	Time				

Figure 2.3: LTE OFDMA Downlink Resource Assignment in Time and Frequency



CHAPTER 3

Simulation Platform

3.1 Simulation Assumptions

The simulation assumptions consists of the parameters about BSs, MSs, and the propagation channel. In the realistic wireless channel, the signal will be deteriorated due to three reasons: path loss, shadowing, and fading. We will introduce the analytical models for each effect and consider thermal noise. With the bandwidth and the noise figure, we can estimate the received noise power.

The simulation scenarios are based on assumptions adopted by the IEEE 802.16 standards as shown in Table 3.1. Performance metrics considered in this thesis include the SINR, throughput, and fairness [15], [8], [14].

3.2 Path Loss Model

According to IEEE 802.16j evaluation methodology [9], path loss (PL) depends on distance d , carrier frequency f and antenna height. There are two regions of d . When $d \leq d_0$, it is the line of sight (LOS) situation. PL only depends on d . On the other hand, for $d > d_0$, it is the non-LOS situation. We also consider f and antenna height. This model is suitable for the sub-urban macro cell propagation environments.

Table 3.1: Simulation Assumptions

Parameter	Value	Parameter	Value
Carrier Frequency	2.5 GHz	Cell Structure	Wrap Around 19 Cells
BS to BS Distance	1.732 Km	Temperature	20°C
Path Loss Model	Sec 3.2	Shadowing Model	Sec 3.3
Fading Channel	Sec 3.4	Thermal Noise	Sec 3.5
BS Height	32 m	BS Tx Power	46 dBm
MS Height	1.5 m	MS Tx Power	23 dBm
Scheduling	Round Robin	Antenna Pattern	Sec 3.7
FFT Size	1024 points	Sampling Frequency	11.2 MHz

$$PL(dB) = \begin{cases} 20 \log\left(\frac{4\pi d}{\lambda}\right), & \text{if } d \leq d_0 \\ A + 10 \cdot \gamma \cdot \log\left(\frac{d}{d_0}\right) + \Delta PL_f + \Delta PL_h, & \text{if } d > d_0 \end{cases}$$

where:

$$A = 20 \cdot \log\left(\frac{4\pi d'_0}{\lambda}\right);$$

$$\gamma = \left(a - b \cdot h_b + \frac{c}{h_b}\right);$$

$$d_0 = 100m;$$

$$d'_0 = d_0 \cdot 10^{-\frac{\Delta PL_f + \Delta PL_{ht}}{10\gamma}};$$

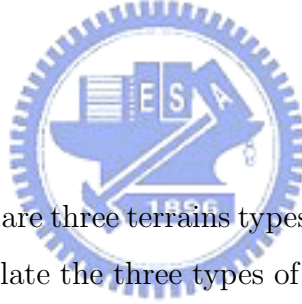
$$\Delta PL_f = 6 \log\left(\frac{f(MHz)}{2000}\right);$$

$$\Delta PL_{ht} = -20 \log\left(\frac{h_t}{3}\right);$$

d = distance between BS and MS;

h_b = height of BS;

h_t = height of MS.



(3.1)

In Table 3.3, there are three terrain types, including hilly and flat terrain. This path loss model can simulate the three types of terrains by changing the parameters: a , b , and c . The value a , b , and c in (3.1) are listed in Table 3.2. In this thesis, we consider the terrain type A, i.e. hilly terrain with moderate-to-heavy tree density. The effect of distance on path loss for terrain type A is shown in Fig. 3.1.

Table 3.2: Path Loss Parameters in Different Types of Terrains

Model Parameter	Terrain Type A	Terrain Type B	Terrain Type C
a	4.6	4	3.6
b	0.0075	0.0065	0.005
c	12.6	17.1	20
σ_μ	10.6	9.6	8.2

Table 3.3: Types of Terrains

Terrain Type	Description
A	Hilly terrain with moderate-to-heavy tree density
B	Intermediate path-loss condition
C	Flat terrain with light tree densities

3.3 Shadowing Model

According to IEEE 802.16j evaluation methodology [9], shadowing is a log-normal random variable with standard deviation σ . Note that σ is related with distance d in (3.2).

$$\sigma(d) = \sigma_{\mu} \left[1 - e^{-\frac{|PL(d) - PL_{fs}(d)|}{4}} \right] + 1.5, \quad (3.2)$$

where: σ_{μ} is the maximum standard deviation; $PL(d)$ is the mean path loss in dB; $PL_{fs}(d)$ is the free space path loss in dB.

Similar to path loss, we consider the shadowing in LOS or NLOS based on the distance. When $d \leq d_0$, LOS situation is considered. $PL(d)$ is equal to $PL_{fs}(d)$ and the shadowing standard deviation is a constant 1.5. As d increases, $\sigma(d)$ increases but will be saturated at $\sigma_{\mu} + 1.5$.

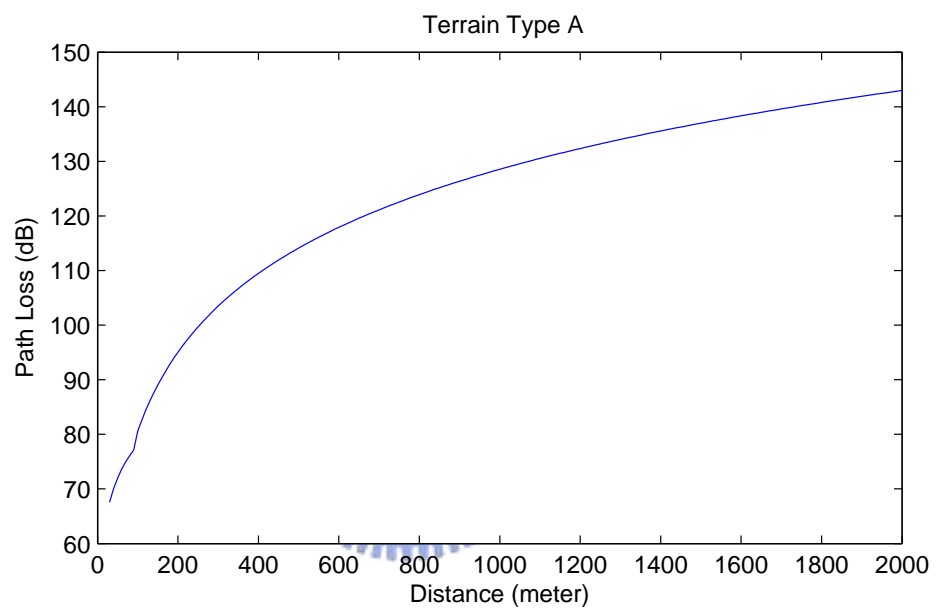


Figure 3.1: Effect of Distance on Path Loss in the Terrain Type A of Propagation Model of IEEE 802.16 WiMAX

3.4 Frequency Selective Fading Channel

According to IEEE 802.16a contribution [6], the frequency selective fading channel is described as three delayed taps in the time domain. The i_{th} tap A_i is a Ricean random variable in (3.3). After sampling and doing FFT, we can obtain the channel frequency response as:

$$A_i = R + M, \tag{3.3}$$

where R is a Rayleigh random variable and M is the LOS component.

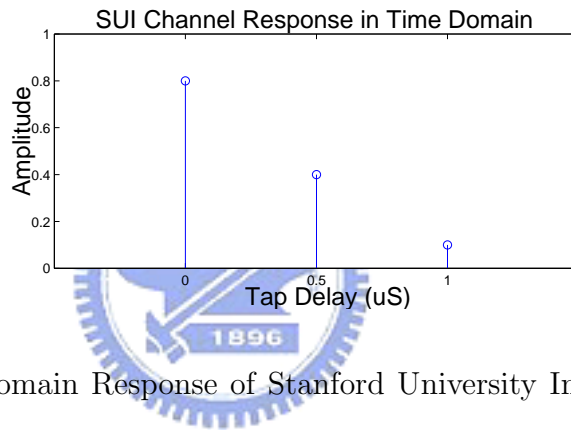


Figure 3.2: Time Domain Response of Stanford University Interim Channel Model (SUI)

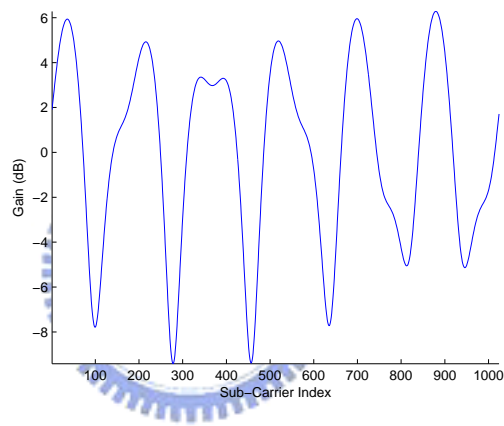


Figure 3.3: Frequency Domain Response of SUI-3 Model

3.5 Thermal Noise Budget

The thermal noise is considered as additive white gaussian noise (AWGN). The noise power density N_0 is proportional to absolute temperature T . That is:

$$N_0 = K \times T \text{ and } K = 1.38 \times 10^{-23} \text{ (} m^2 k g s^{-2} K^{-1} \text{)} , \quad (3.4)$$

where K is the Boltzman constant. The thermal noise density in $20^\circ C$ is:

$$10 \log(1.38 \times 10^{-23} \times (273 + 20)) + 30 = -173.9 \frac{dBm}{Hz} , \quad (3.5)$$

Consider a bandwidth of 10MHz and the noise figures are 5 dB/ 7 dB in BS/ MS. The thermal noise power in MS will be:

$$-173.9 + 7 + 10 \log(10^7) = -96.9 dBm , \quad (3.6)$$

3.6 Wrap Around Scheme

In the IEEE 802.16m evaluation methodology [5], the wrap-around scheme is formed with 7 clusters and each cluster consists of 19 cells. In Fig. 3.4, only 19 cells in the middle are generated and the other interference cells are wrapped from the 19 cells. Each cell in the middle cluster can see two layers of interference sources. The merit of wrap around is to save the computation time and memory space in the simulation. The interference sources can be simulated correctly.

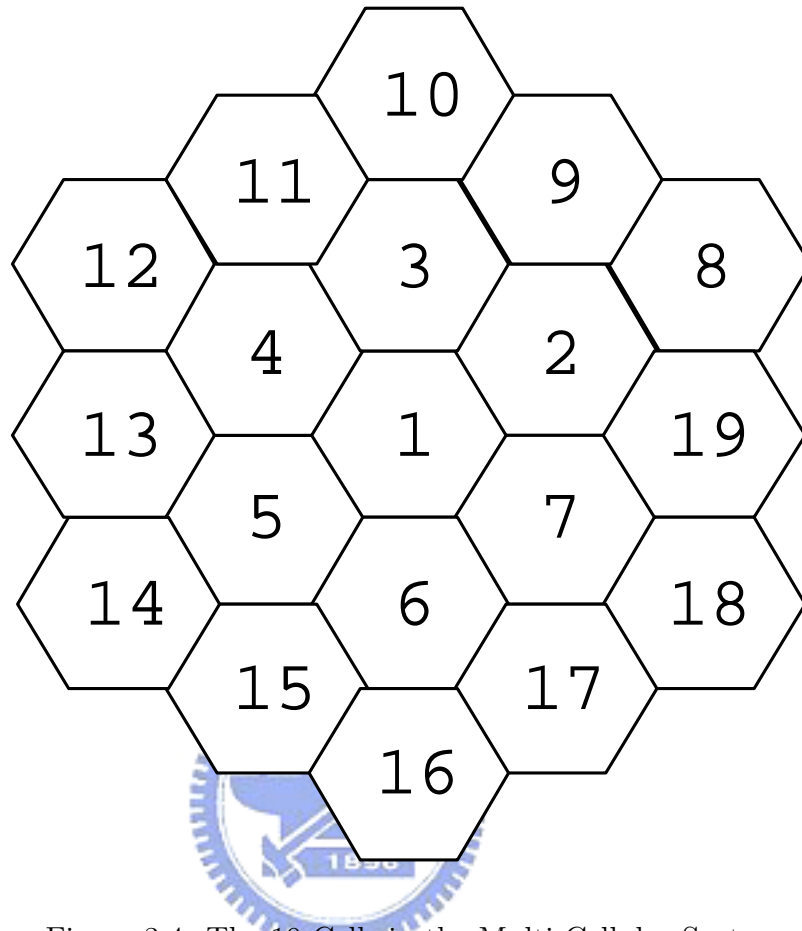


Figure 3.4: The 19 Cells in the Multi-Cellular System

3.7 Directional Antenna Pattern

In the IEEE 802.16m evaluation methodology [5], a cell will be divided into three sectors and the BS has three directional antenna, respectively. In this thesis, we will discuss three types of antenna patterns. The default antenna pattern is called the Wide-Beam Trisector Cell with Pentagon-Shaped Sector type. The other two types of directional antenna are Wide-Beam Trisector Cell with Diamond-Shaped Sector and Narrow-Beam Trisector Cell types, respectively.

3.8 Computation of per Sub-channel Effective SINR

The effective SINR in a sub-channel is related to the SINR in total sub-carriers. In [15], some metrics for SINR in the multi-carrier case are introduced, such as exponentially effective SINR map (EESM), effective code rate map (ECRM), and mean instantaneous capacity (MIC).

In this thesis, we adopt the MIC method. Denote γ the effective SINR in a sub-channel, and γ_i the SINR in a sub-carrier. Based on the Shannon's information capacity rule, the capacity of a sub-channel is the summation of the capacity of the sub-carriers. Let N_s be the number of sub-carriers in a sub-channel. Then we can have:

$$\log_2(\gamma + 1) = \sum_{i=1}^{N_s} \frac{1}{N_s} \log_2(\gamma_i + 1) , \quad (3.7)$$

$$\gamma = 2^{\frac{1}{N_s} \sum_{i=1}^{N_s} \log_2(\gamma_i + 1)} - 1 , \quad (3.8)$$

3.9 Capacity Evaluation

Fig. 3.5 shows the link level throughput v.s. SINR for the IEEE 802.16 OFDM mode with seven adaptive modulation coding schemes (MCS) [8]. The evaluation is based on OFDM FFT size of 256 and 3.5 MHz bandwidth. The capacity can be obtained from SINR and linear interpolation. PHY parameters used in this thesis and in [8] are listed in Table 3.4.

Table 3.4: PHY Parameters in This Thesis and in [8]

Parameters	Bandwidth	FFT Size	Number of Sub-channel
This Thesis	10 MHz	1024	30
[8]	3.5 MHz	256	1

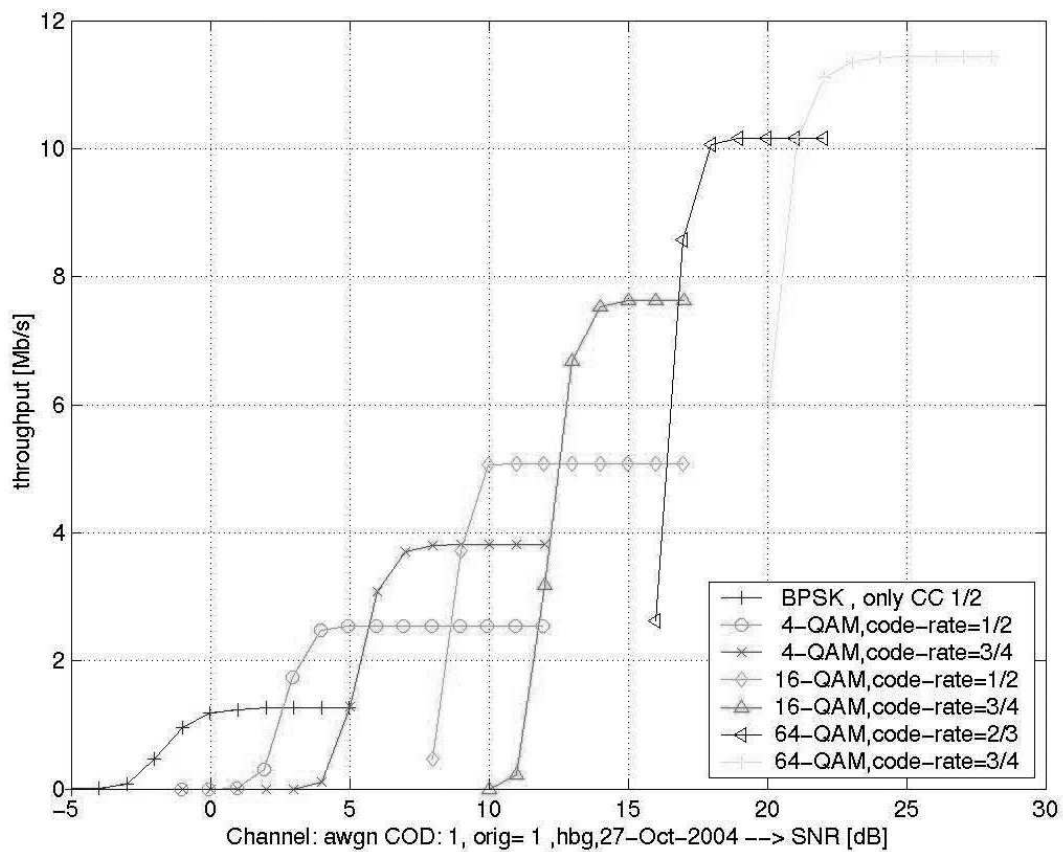


Figure 3.5: Effect of Various SINR on the Throughput with Different Modulation and Coding Schemes

3.10 Fairness Index

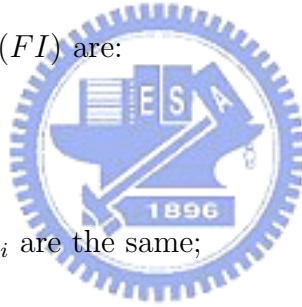
Fairness is an important issue. If the system is on fair, the poor-throughput users will be very unconformable and may exist the network and join another network soon. It's not a good idea if the network provider want to develop their business.

According to [14], we use the Jain's fairness index to evaluate the fairness among the users in the cell. The fairness index (FI) among variables x_1, x_2, \dots, x_n is defined as (3.9). The (FI) is related to the the first moment and second moment.

$$FI(x_1, x_2, \dots, x_n) = \frac{(\sum_{i=1}^n x_i)^2}{n \sum_{i=1}^n x_i^2} , \quad (3.9)$$

The properties of (FI) are:

1. $0 \leq FI \leq 1$;
2. $FI= 1$ when all the x_i are the same;
3. Larger FI implies fairer.



For example, if all the x_i are the same, i.e. $x_i = 1$, this is the fairest situation. (FI) is one, i.e.

$$FI(x_1, x_2, \dots, x_n) = \frac{(\sum_{i=1}^n 1)^2}{n \sum_{i=1}^n 1^2} = \frac{n^2}{n \times n} = 1 , \quad (3.10)$$

CHAPTER 4

Effects of the Interference Averaging Technique: Sub-carrier Permutation

4.1 Types of Sub-carrier Permutation

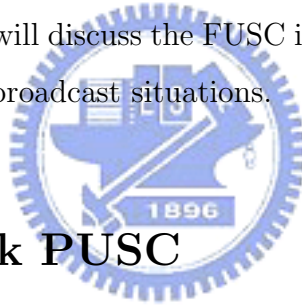
Permutation is the way to allocate the sub-carriers in a sub-channel. There are two types of permutations: Continuous sub-carrier and randomly distributed sub-carrier permutation methods, as shown in Table 4.1. The usage of sub-channel can save the size of the header in MAC layer. For a 1024-point FFT, we need 10 bits to allocate a sub-carrier. For a 64-QAM modulation, there are only 6 information bits in a sub-carrier. The huge size for indexing sub-carriers is not practical. For a sub-channel with 48 sub-carriers, one can only use 5 bits to index the total 30 sub-channels.

In the IEEE 802.16m evaluation methodology [5], the PUSC permutation is suggested. PUSC is used together with the Wide-Beam Trisector Cell with Pentagon-Shaped Sector antenna pattern. We will discuss the details of the antenna pattern in Chapter 6. There are six major groups and each group has its own pilots. BS sends only two major groups into the air from each sector. For comparison, Band AMC is also discussed as the adjacent type permutation.

Table 4.1: Permutation Types in WiMAX

Sub-Carrier Permutation Type	Example
Randomly Distributed	PUSC (Partial Usage of the Sub-Channels) OPUSC (Optional PUSC) FUSC (Full Usage of the Sub-Channels) OFUSC (Optional FUSC)
Continuous	Band AMC (Band Adaptive Modulation and Coding)

FUSC is suitable for the broadcast messages since FUSC uses the whole band of bandwidth. The pilots are common among all the sub-channels. All the sectors must sent all the sub-carriers and pilots into the air. Usually FUSC is used with omnidirectional antenna. We will discuss the FUSC in Chapter 6, which is omnidirectional antenna and suitable in broadcast situations.



4.2 Down Link PUSC

4.2.1 Symbol Structure

In the IEEE 802.16e standard [10], an OFDMA PUSC symbol contains guard sub-carriers, dc carrier, and clusters. The symbol structure is shown as Fig. 4.1. The frequency of dc carrier is the same as carrier frequency. We can't transmit data at dc carrier. The guard sub-carrier is designed to avoid the leakage from the adjacent frequency bands. There are 60 clusters and 720 data carriers in an OFDMA symbol.

The structure of cluster has two phase according to odd or even OFDMA symbol numbers. Pilot sub-carriers appear at different locations in odd or even OFDMA

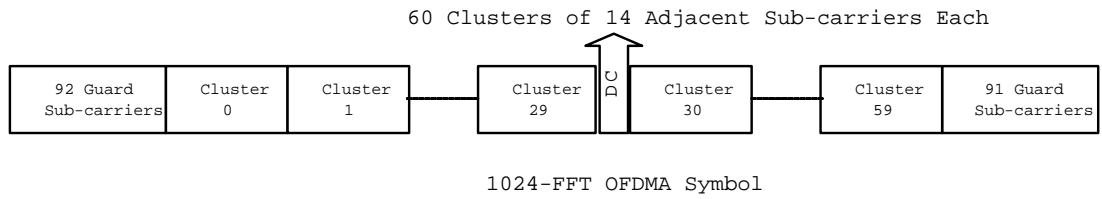


Figure 4.1: PUSC Symbol Structure

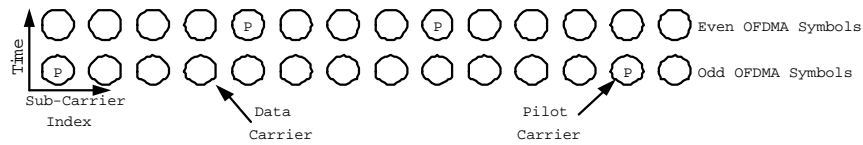


Figure 4.2: PUSC Cluster Structure

symbols. The cluster structure is shown as Fig. 4.2. This is helpful in synchronization because of the regular structure of the pilots. It's good for channel estimation since we can learn four pilots in a cluster. In Table 4.2, 30 sub-channels can be divided into 6 major groups. Two groups are used in each sector. The sub-channels in one major group corresponded to one specific set of clusters.

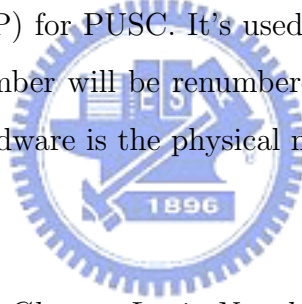
4.2.2 Renumbering and Permutation Base Assignment

During the PUSC channel assignment, the renumbering occurs twice. Renumbering is depended on the parameter: permutation base. For example, in Fig. 4.3 there are 60 clusters in an OFDMA PUSC symbol. The clusters will be renumbered and collected into 6 major groups. In Major Group 1, there are 96 data sub-carriers after removing the pilots. Now we do the renumbering and collection again. The 96 sub-carriers will be renumbered and collected into 4 sub-channels.

Table 4.2: PUSC Sub-Channels

Major Group	Sub-Channel Range	Cluster Range	Sector
0	0-5	0-11	0
1	6-9	12-19	0
2	10-15	20-31	1
3	16-19	32-39	1
4	20-25	10-51	2
5	26-29	52-59	2

DL_PermBase is an integer ranging from 0 to 31, which can be indicated by down-link map (DL_MAP) for PUSC. It's used in distributing the clusters and sub-carriers. The cluster number will be renumbered based on DL_PermBase. In (4.1), the actually index in hardware is the physical number.



$$\text{Cluster Logic Number} = \text{Renumbering Sequence}$$

$$((\text{Cluster Physical Number} + 13 \cdot \text{DL_PermBase}) \bmod N_{\text{clusters}}) \quad (4.1)$$

We define two types of permutation usage as shown in Table 4.3. In type 0, various BSs can use the same permutation base. In type 1, permutation bases are different among various cells.

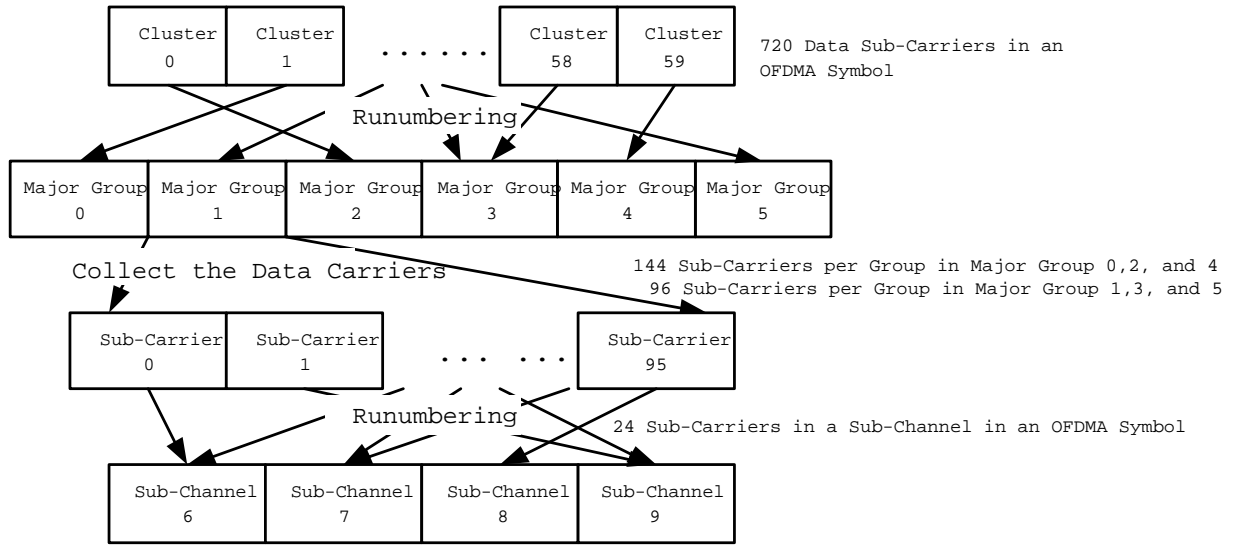


Figure 4.3: PUSC Sub-Channel Generation

Table 4.3: Permutation Base

Assignment Type	Permutation Base Value Among Different Cells
Type 0	Same
Type 1	Random

4.2.3 Results of Locations of Sub-carriers in PUSC

Fig. 4.4 shows the sub-carriers for different sub-channels when $DL_PermBase = 0$ in (4.1). We can see that the six major groups can be separated in frequency domain. Fig. 4.5 shows the effects of different Permutation Base. We can see that the frequency segment can be done in PUSC Type 0. However, the frequency segmentation is not achievable when the Permutation Base is different even though we use the same 7th sub-channels in different cells.

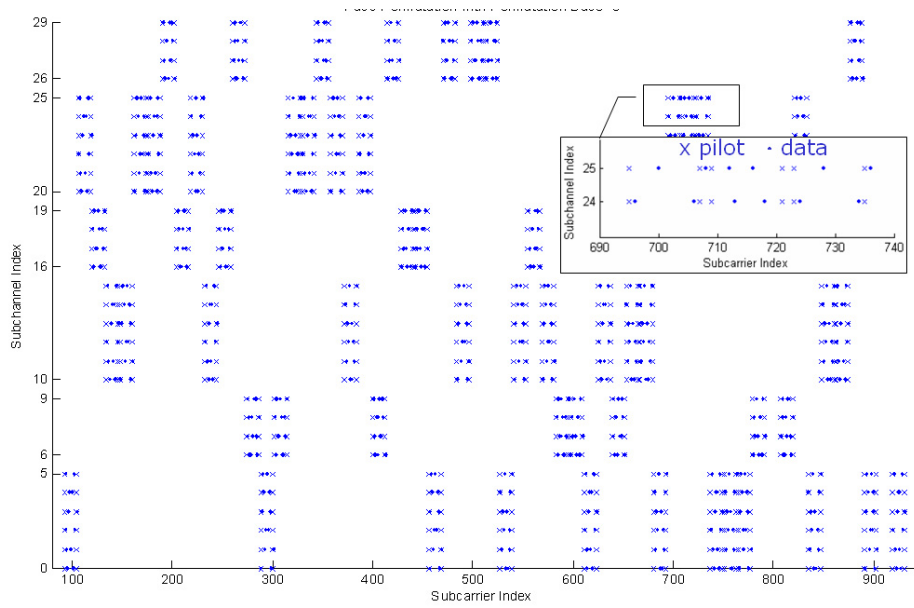


Figure 4.4: Sub-Carriers of Different Sub-Channels when $DL_PermBase = 0$

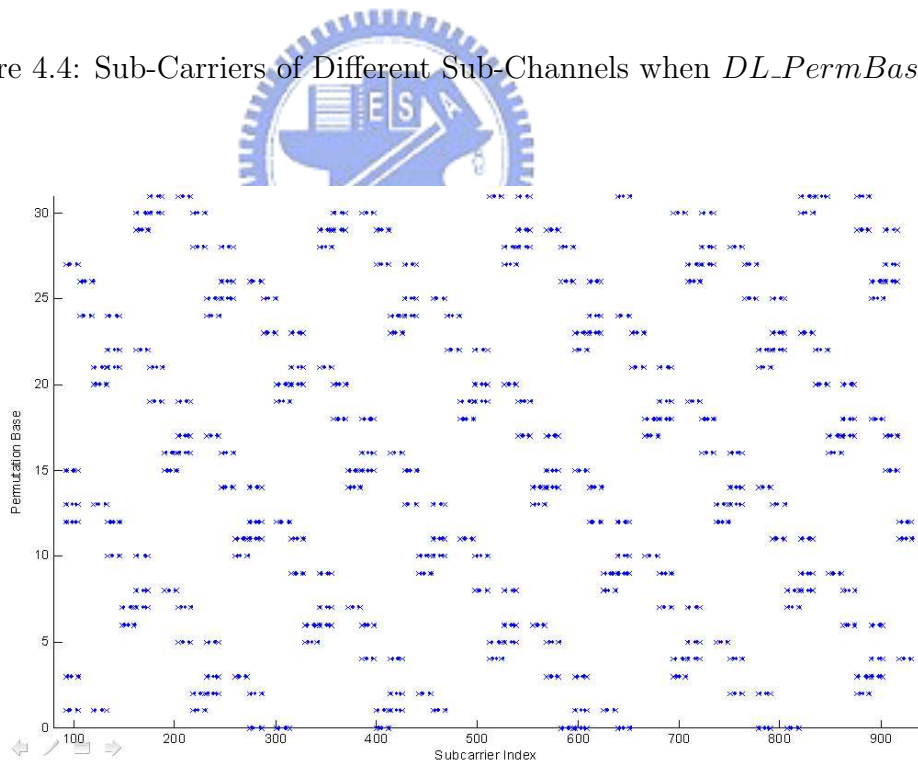


Figure 4.5: Sub-Carriers in the 7th Sub-Channel for Various Value of $DL_PermBase$

4.3 Down Link FUSC Permutation

FUSC is another important member of randomly distributed sub-carrier permutation method. A FUSC symbol is constructed using guard carriers, pilots, data carriers, and the DC carrier. In a 1024-FFT OFDMA symbol, there are 768 data carriers and 82 pilots. All the pilots and data carriers are distributed in the whole frequency band. It's suitable for omnidirectional antenna. The symbol structure of FUSC is shown in Fig 4.6.

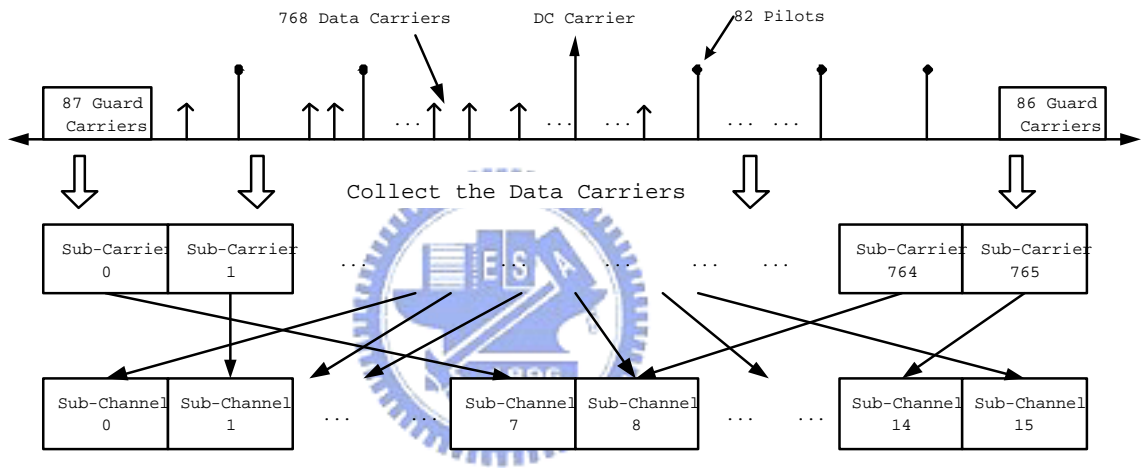


Figure 4.6: FUSC Symbol structure and Sub-Channel Generation

4.4 Down Link Band AMC Permutation

Similar to PUSC, an OFDMA Band AMC symbol contains guard sub-carriers, dc carrier, and bins. A bin contains 8 data carriers and 1 pilot carrier. In 1024-FFT mode, there are 96 bins in an OFDMA symbol. The structure of a bin and Band AMC sub-channel is shown in Fig. 4.7.

There are 4 types in Band AMC. Each type occupies different OFDMA symbol number and consecutive bins in the same time. Table 4.4 shows the details. If the coherence time of the channel is long enough, we can choose the Band AMC type in larger OFDMA symbols.

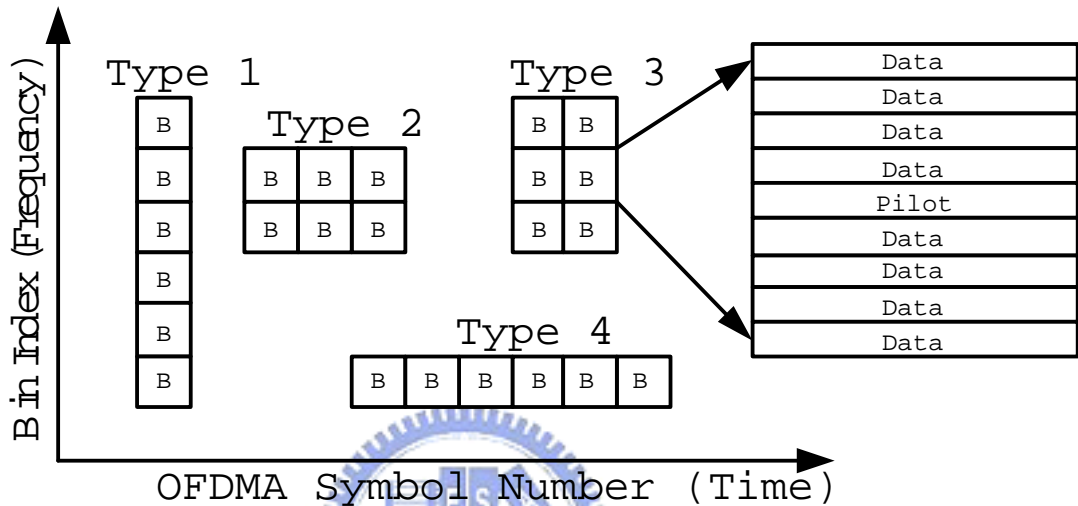


Figure 4.7: Band AMC Bin and Sub-Channel Structure

Table 4.4: Band AMC Sub-Channels

Type	Bins and Symbols	Sub-channels
Type 1	6 bins \times 1 OFDMA symbol	16
Type 2	2 bins \times 3 OFDMA symbols	48
Type 3	3 bins \times 2 OFDMA symbols	32
Type 4	1 bin \times 6 OFDMA symbols	96

Because the number of sub-carriers in a PUSC sub-channel is 24, I choose Band AMC Type 3 in this report for comparison. In this thesis, only 10 sub-channels per sector are used and the total number of sub-channels is 30.

4.5 Numerical Results

In this section, we concern about the cumulative distribution function (CDF) of users' received SINR. We focus on the 90% tile because it implies the quality of the poor users in the system. The users who get poor throughput usually complain and need help. The CDF is shown in Fig. 4.8

The traffic load is defined as the load of the adjacency cells. In this thesis, we close some proportion of sub-channels to simulate the traffic load. This is because that we don't simulate the MAC layer. Table 4.5 and Fig. 4.9 show the results the 90% tile of users.

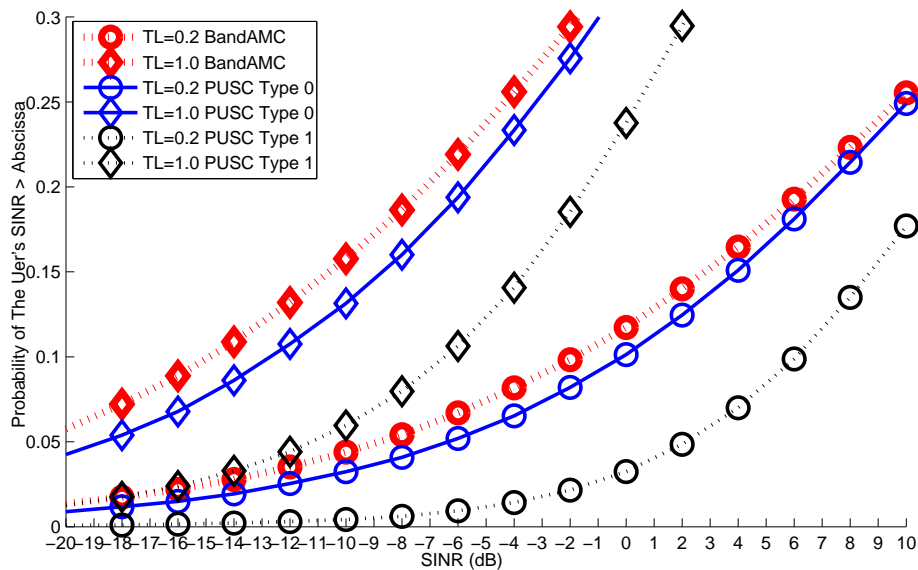


Figure 4.8: The Users' SINR in PUSC Type 0, PUSC Type 1, and Band AMC

Table 4.5: The 90% Tile of Users' Received SINR for Fig. 4.8

Type	TL=0.2	TL=0.6	TL=1.0
PUSC Type 0	0.7135	-7.4572	-11.1309
PUSC Type 1	6.2728	-1.7477	-5.7498
Band AMC	-1.1269	-9.9525	-13.7623

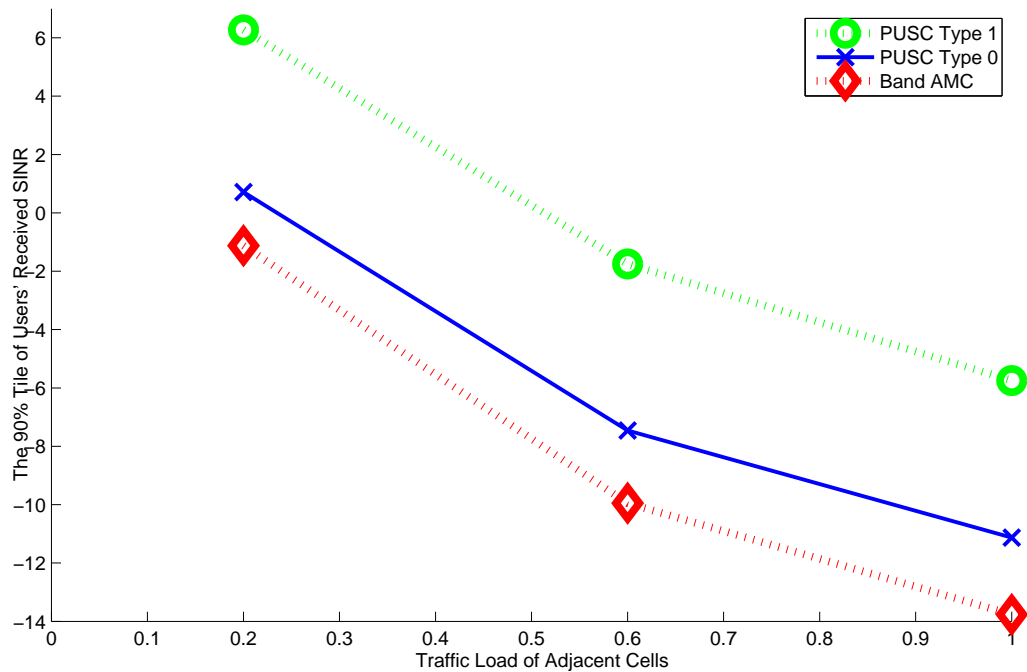


Figure 4.9: The 90% Tile of Users' Received SINR Figure

4.5.1 Comparison of PUSC and Band AMC

In PUSC Type1, the 90% tile users improve 7.8 dB SINR under traffic load = 0.2 compared to Band AMC. This is because that the interference is averaged by the permutation in PUSC. If we choose the PUSC Type 0, users can get more 1.8 dB

further. We can say that the PUSC get the merit from the frequency selective fading channel. PUSC Type 0 needs the additional cooperation among cells but gets poorer performance than PUSC Type 1. It's not suggested in this thesis.

4.5.2 Comparison of Distributed or Contiguous Sub-Carriers

Fig. 4.10 shows how the distributed permutation can ease the co-channel interference. In distributed method PUSC, only some sub-carrier will suffer co-channel interference, and the signal may be recovered by some coding methods. However, in contiguous permutation Band AMC, if there is an interference source nearby, all the sub-carriers will suffer severe co-channel interference.

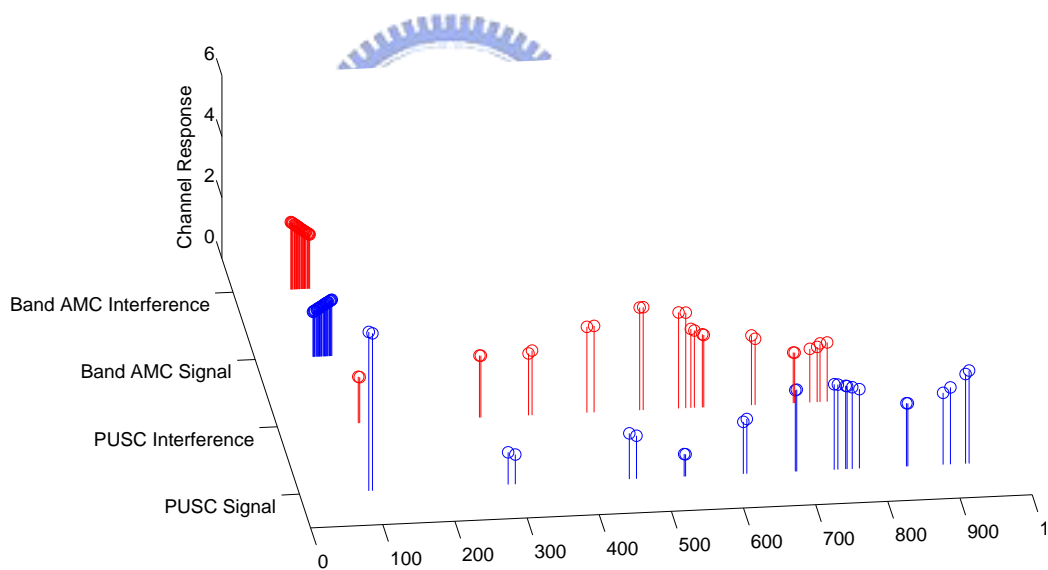


Figure 4.10: Comparison of Randomly Distributed and Contiguous Subcarrier Permutations

CHAPTER 5

Effects of the Interference Avoidance Technique: Frequency Reuse

5.1 Types of Frequency Reuse

5.1.1 Regular Frequency Reuse

The frequency reuse can change the distance of co-channel interference source from the other cell. The larger distance induces smaller interference. The concept of reuse was proposed in 1979 [11]. The reuse factor N can be obtained from (5.1) and (5.2). The total bandwidth W is divided into N parts, and the available bandwidth of each user is $\frac{W}{N}$.

$$N = i^2 + ij + j^2 \quad (5.1)$$

where i, j are non-negative integers.

$$\frac{D}{R} = \sqrt{3N} \quad (5.2)$$

where D is the frequency reuse distance and R is the cell radius.

In this thesis, we would like to evaluate the $N= 1, 3, 4,$ and 7 . Fig. 5.1 illustrates the locations of interference cells related to the center cell when $N= 3, 4,$ and 7 . The basic unit is the cell, and cells with the same index number use the same frequency band. N cells is combined as a cluster, and the available frequency band of these cells will not be duplicate. Hence, there is no intra-cluster interference within a cluster.

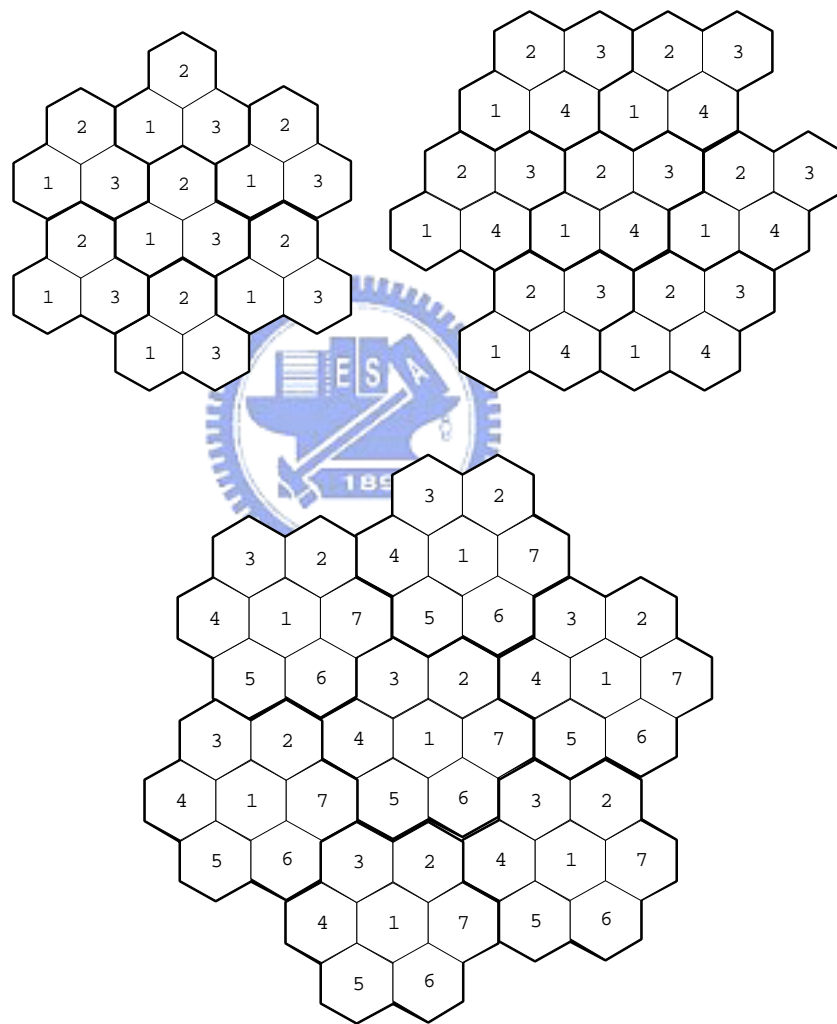


Figure 5.1: Cell Planning when Reuse Factor $N= 3, 4,$ and 7

5.1.2 Fractional Frequency Reuse

In [12], the fractional frequency reuse (FFR) can be applied in the WiMAX systems. A cell will be divided into two parts: inner circle and outer ring. Fig. 5.2 illustrates an example of FFR scheme with 3 cells. The users in outer ring in each cell use frequency: $F1$, $F2$, and $F3$, respectively, and the users in inner circle use the frequency band $F0$.

Comparing to reuse factor $N=1$, i.e. there is no outer ring in the system, the FFR will induce: 1) The co-channel interference of the outer users can be reduced; 2) The usable bandwidth is less. We will discuss the two effects in this thesis.

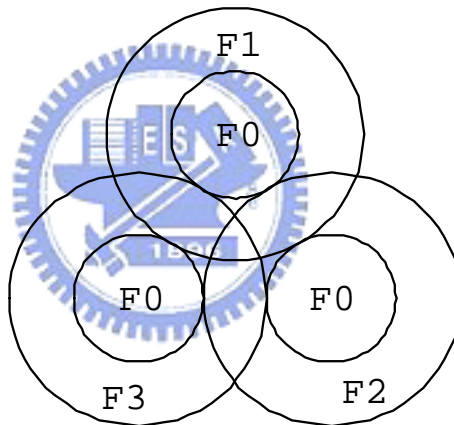


Figure 5.2: Fractional Frequency Reuse

5.1.3 Achievable FFR Factors

We assume that the reuse factor N in inner circle is not smaller than the reuse factor N in the outer ring. The achievable FFR schemes in this thesis are listed in Table 5.1. The ratio p is defined as (5.3).

$$p = \frac{\text{Number of Channels in Outer Ring}}{\text{Number of Channels in Outer Ring and Inner Circle}} \quad (5.3)$$

The FFR factor is calculated in (5.4). In this thesis, we will choose some values from Table 5.1. The reuse factor is:

$$\text{Reuse Factor} = \frac{\text{Number of Channels}}{\text{Number of Assigned Channels per Cell}} \quad (5.4)$$

$$\text{Reuse Factor} = p \times RF_{\text{Outer Ring}} + (1 - p) \times RF_{\text{Inner Circle}} \quad (5.5)$$

For example, if $p = \frac{3}{8}$, $RF_{\text{inner}} = 1$, and $RF_{\text{outer}} = 3$, we can assume that the number of assigned channels per cell is 8. The number of channels in inner circle/outer ring are 3/5. The total number of channels in the system is $3 \times 3 + 5 \times 1 = 14$. Finally, the reuse factor is $\frac{14}{8} = 1\frac{3}{4}$.

5.2 Inner Circle and Outer Ring User Decision

In Section 5.1.2, the shape of the inner circle is a round shape. However, the round shape is not reasonable in this thesis because of the antenna gain, cell structure, and

Table 5.1: FFR Values

RF Inner Circle	RF Outer Ring	$p = \frac{1}{8}$	$p = \frac{3}{8}$	$p = \frac{4}{8}$	$p = \frac{5}{8}$	$p = \frac{6}{8}$
1	1			1		
1	3	$1\frac{1}{4}$	$1\frac{3}{4}$	2	$2\frac{1}{4}$	
1	4	$1\frac{3}{8}$	$2\frac{1}{8}$	$2\frac{1}{2}$	$2\frac{7}{8}$	
1	7		$3\frac{1}{4}$	4	$4\frac{3}{4}$	
3	3			3		
3	4		$3\frac{3}{8}$	$3\frac{1}{2}$	$3\frac{5}{8}$	
3	7		$4\frac{1}{2}$	5	$5\frac{1}{2}$	6
4	4			4		
4	7		$5\frac{1}{8}$	$5\frac{1}{2}$	$5\frac{7}{8}$	$6\frac{1}{4}$
7	7			7		

shadowing in the simulation platform of this thesis. Instead, the decision of that the user is in inner circle or outer ring is based on the signal strength of the user. In Fig. 5.4, 20 users are divided into 10 inner users and 10 outer users by their signal strength.

The signal strength is a basic parameter in wireless cellular systems. Fig. 5.3 shows a sample of signal strength in a 2G system. In the IEEE 802.16, the BS and MS can get the signal strength from ranging messages. Signal strength based decision is more reasonable than distance based decision in this thesis. If we use the distance in decision, the received power of users of inner circle and outer ring are not the same due to the directional antenna. Another reason is that it's hard for BS to measure the distance between BS and MS practically.



Figure 5.3: Signal Strength in a 2G System Cell Phone

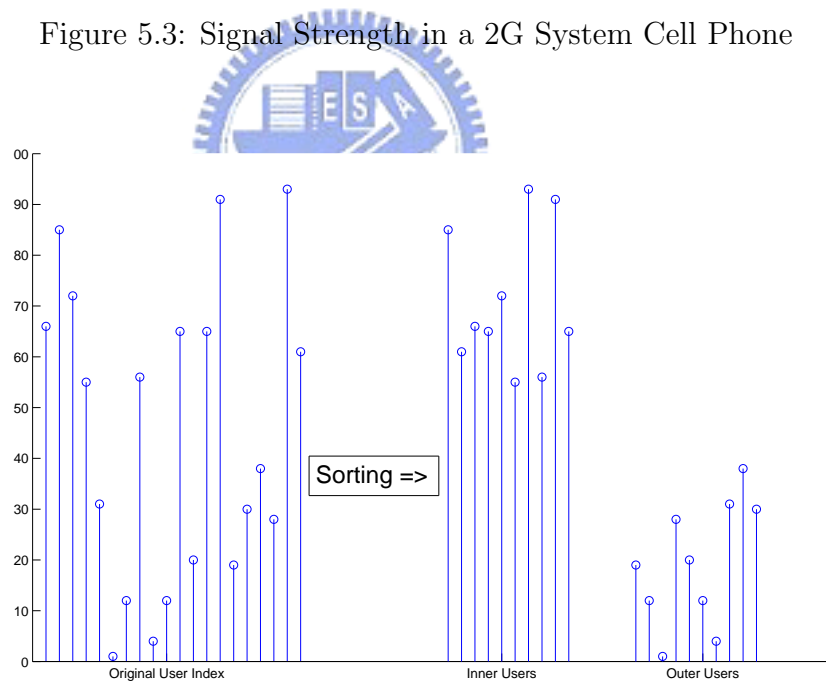


Figure 5.4: Selection of Inner and Outer Users by Sorting on Received Power Strengths

5.3 Permutation Base Assignment in Frequency Reuse

Similar to Chapter 4, the assignment of the Permutation Base will affect the system performance under FR planning. Compared to Table 4.3, the cluster is a new consideration in Table 5.2. Fig. 5.5 shows the difference between PUSC Type 0 and Type 1 when $RF=3$. In order to divide the frequency band into partitions, Permutation Base in a cluster must be the same otherwise the intra-cluster interference can not be avoided. In PUSC Type 0, the users suffer interference only from one cell from the adjacent cluster. In PUSC Type 1, the users suffer interference from all the cells from the adjacent clusters, but the strength of the interference from each cell is less than that in PUSC Type 0.

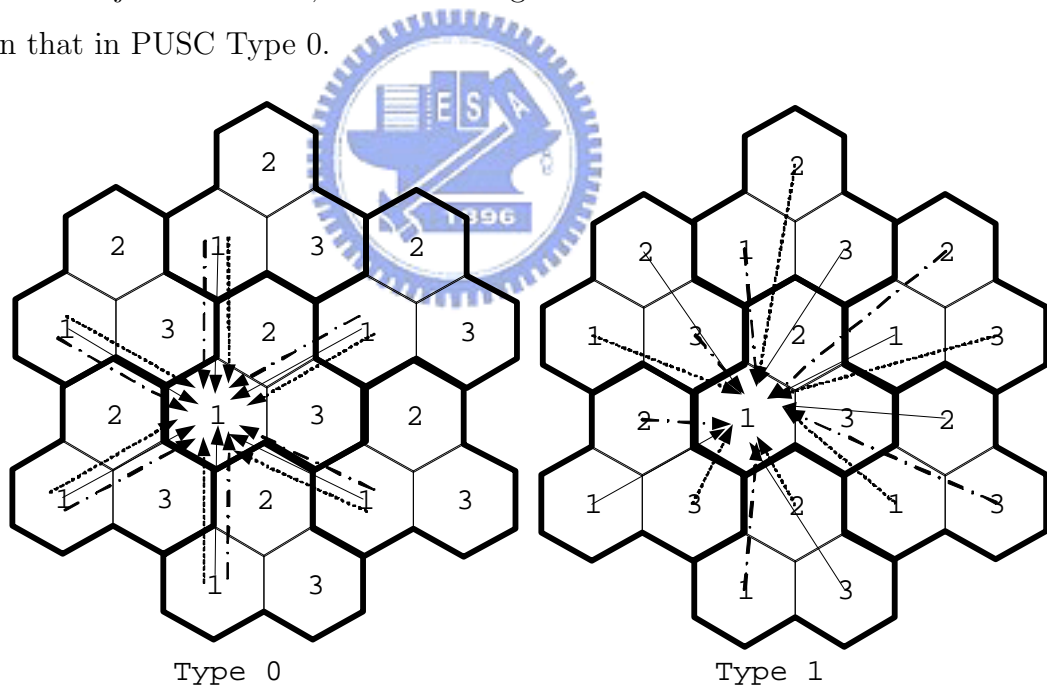


Figure 5.5: Interference Sources of Different Permutation Base Assignment in Reuse Factor $N=3$

Table 5.2: Permutation Base Assignment with Frequency Reuse

Assignment Type	Permutation Base Among Different Clusters
Type 0	Same
Type 1	Random

5.4 Relation of Frequency Reuse and Throughput

Fig. 5.6 shows the trends of reuse factor and throughput. In this thesis, the power of interference strongly depends on the distance with path loss exponent γ . By (5.2), we get the relationship between SINR and N in (5.6). The SINR is increasing as reuse factor increasing. In Siemens [8], users can use the adaptive MCS in various SINRs. This means the higher SINR, users can get higher throughput.

However, the usable channels of users will shrink as reuse factor increasing in (5.7). This is because the usable bandwidth will be divided into some parts. There are trade-offs between these two effects. We will see these two parts in the numerical results.

$$SINR \propto \frac{1}{Interference\ Power} \propto (R\sqrt{3N})^\gamma \propto N^{\frac{\gamma}{2}} \quad (5.6)$$

$$Usable\ Channel \propto N^{-1} \quad (5.7)$$

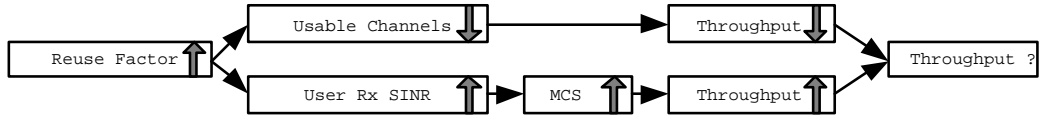


Figure 5.6: Trends of Reuse Factor and Throughput (\uparrow *Increasing*, \downarrow *Decreasing*)

5.5 Numerical Results

5.5.1 Effects of FFR on SINR

Fig. 5.7 shows the effects of the trend as FFR increasing in PUSC Type 0, PUSC Type 1 and Band AMC respectively. The PUSC Type 1 gets the best performance among the three types. The PUSC Type 0 is better than the Band AMC. We can see that as the reuse factor increasing, the users will get higher SINR. The differences of SINR curve are larger when reuse factor is one to three. As the reuse factor increasing, the differences among the curves are smaller.

We also figure out the SINR in FUSC permutation with omnidirectional antenna in Fig. 5.8. We will compare the performance on directional and omnidirectional antenna patterns in Chapter 6.

5.5.2 Effects of FFR on Link Quality

In Fig. 5.9, the 90% tile of users' received SINR will higher as the reuse factor increasing. However, the improvement is not obvious when reuse factor is greater than three. The largest improvement of link quality occurs when the reuse factor is about 1 and 2. PUSC Type 1 gets the best SINR among the schemes because of the randomization of interference sources.

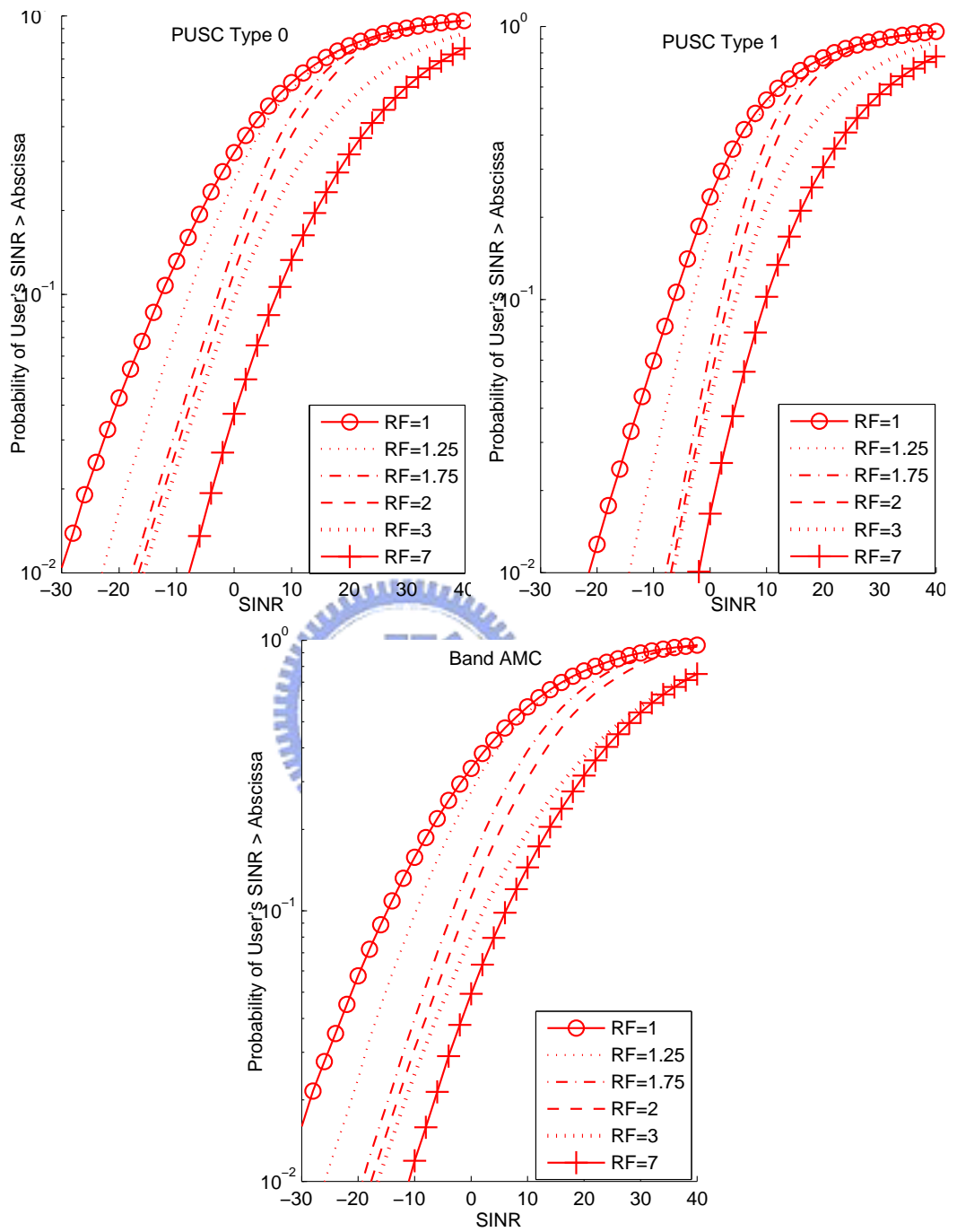


Figure 5.7: CDF of SINR in PUSC Type 0 and Type 1, Band AMC with Varies Reuse Factor in Interference Traffic Load= 100%

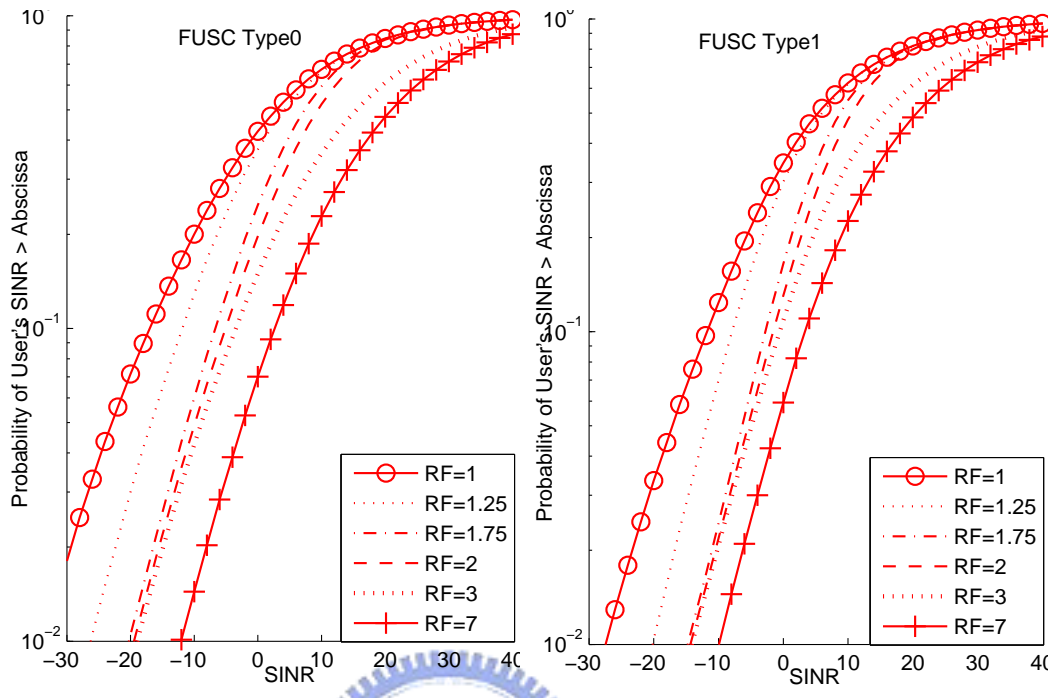


Figure 5.8: CDF of SINR in FUSC Type 0 and Type 1 with Varies Reuse Factor in Interference Traffic Load= 100%

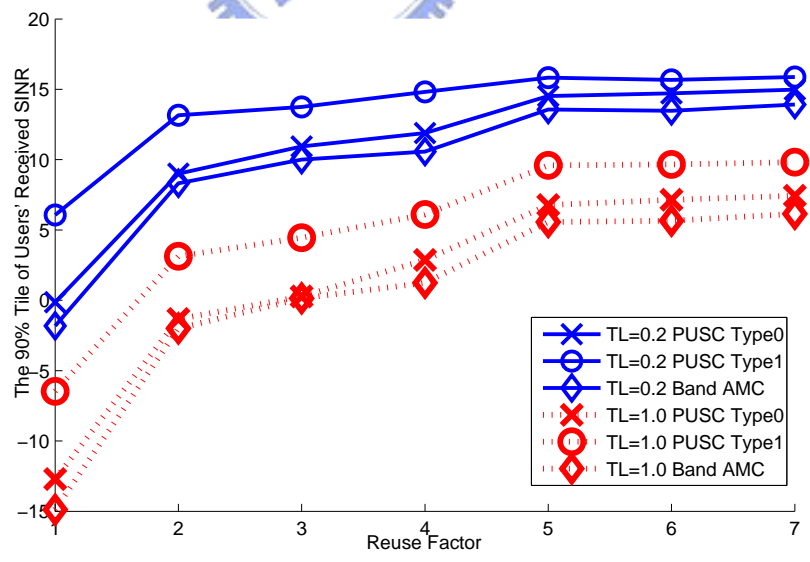


Figure 5.9: The 90% Tile of Users' Received SINR v.s. Reuse Factor

5.5.3 Effects of FFR on Throughput

The reuse factor affects the usable channels and SINR of users. In Fig. 5.6, system throughput may be increasing or decreasing as the reuse factor increasing.

In Fig. 5.10, we can say that the usage of frequency reuse is not useful for the cell total throughput. The decreasing usable channels is the dominate affection in the system. The merit of higher SINR and better MCS does not compensate for loss of throughput due to loss of usable frequency bands.

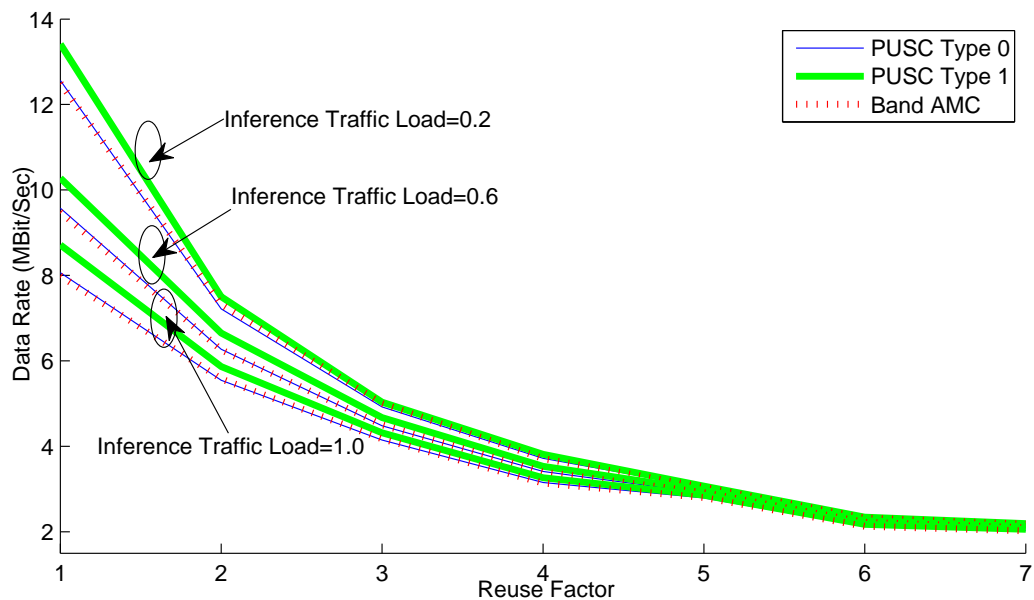


Figure 5.10: Reuse Factor and Cell Capacity

5.5.4 Effects of FFR on Inner Circle and Outer Ring Users

Fig. 5.11 shows the throughput of users in inner circle and outer ring under PUSC Type 1, and Fig. 5.12 shows the fairness of the total users. We can see that the throughput of inner users is the best when reuse factor N is one. The outer user

will suffer poor SINR channels in higher traffic loads (0.6 and 1.0). The sub-carrier permutation is not very powerful for the outer users in these scheme.

However, the outer users get better SINR when reuse factor N is two. Compared to the case $N=1$, the improvements are about 7% to 40%. When reuse factor N is greater than three, the throughput of inner/outer users shrinks as reuse factor N increasing. The fairness is increasing but the improvement is saturated in high reuse factor N . It's not suggested in the environment in this thesis.

In low traffic load (0.2), the SINR is high enough for outer users. So the reuse factor is not very helpful when reuse factor N is greater than 1. There is a large improvement of fairness when N is one to two. The fairness improves as $N > 3$ but the improvement is saturated.

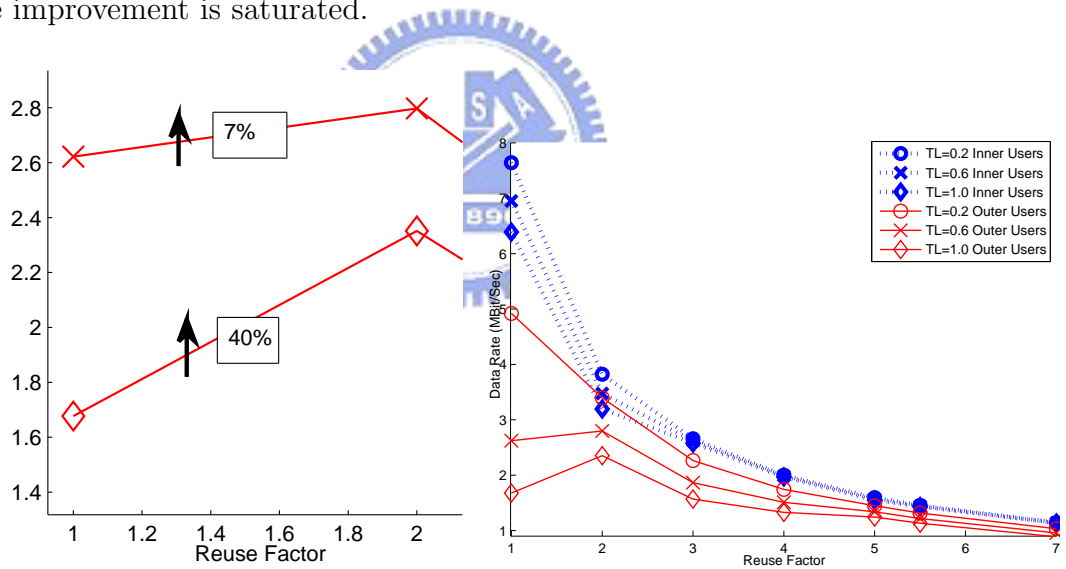


Figure 5.11: The Cell Capacity of Inner/Outer Users in PUSC Type 1

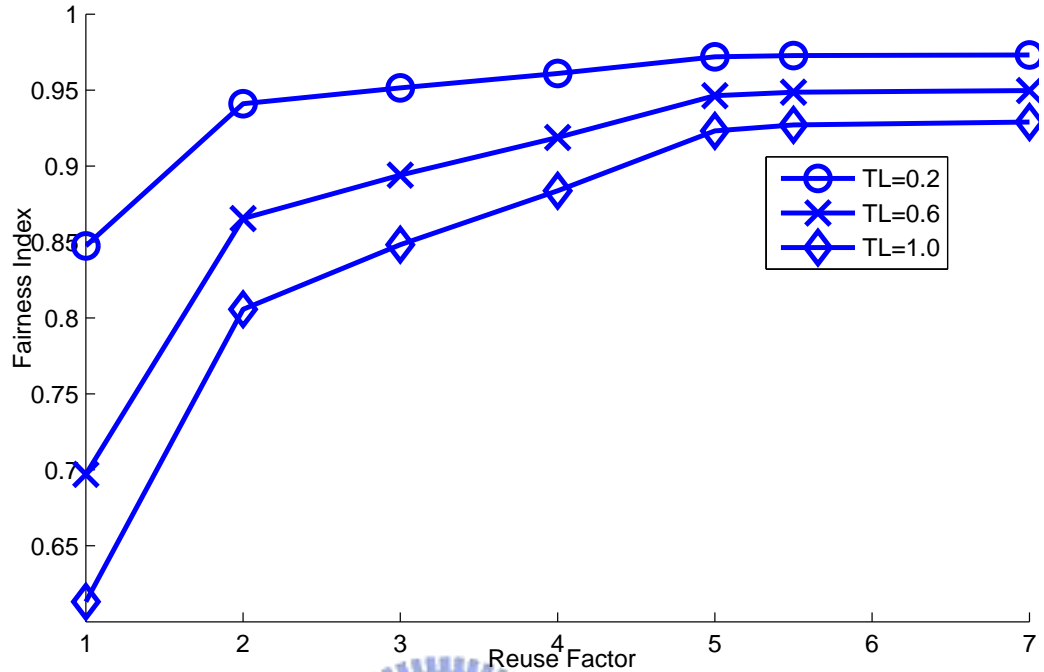


Figure 5.12: The Fairness Index of the Users' Throughput in PUSC Type 1

5.5.5 Comparison of PUSC Type 0 and 1

The distributions of interference sources of PUSC Type 0 and 1 are different. In order to verify the difference, we locate three test users A, B, and C and check the power of interference sources from PUSC Type 0 or 1. The location of users A, B, and C are shown in the left side of Fig. 5.13.

Since some sources of co-channel interference are closer in PUSC Type 1 than in PUSC Type 0, but more sources are further. The result is that the interference power is smaller in PUSC Type 1 in the right side of Fig. 5.13. The performance of PUSC Type 1 will be better than PUSC Type 0 in this thesis.

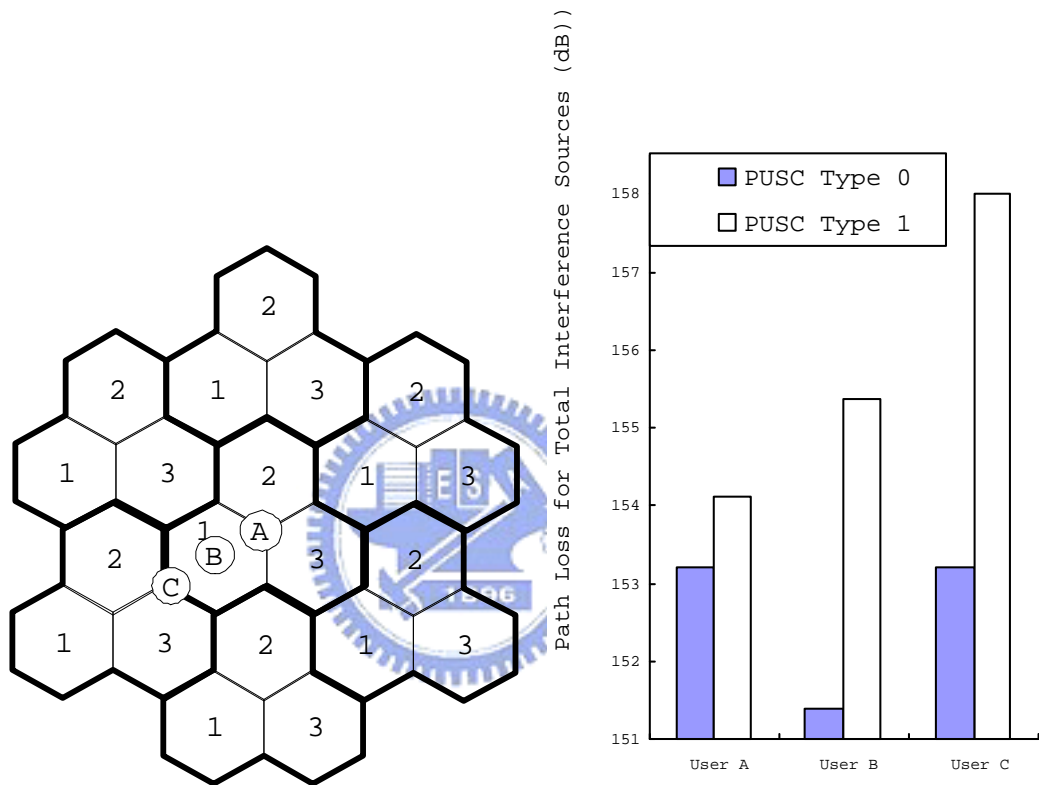


Figure 5.13: The Path Loss of Interference Sources from Different Users A, B, and C

CHAPTER 6

Effects of the Interference Mitigation Technique: Directional Antenna

6.1 Types of Directional Antenna

In this chapter, we'd like to verify different types of directional antennas and the omnidirectional antenna in the multi-cell system. Both in [5] and [7], different antenna patterns are introduced. Three types of antenna patterns involved in this thesis are shown as Table 6.1. [5] suggests the Wide-Beam Trisector Cell with Pentagon-Shaped (WBTC) with type. Wide-Beam Trisector Cell with Diamond-Shaped Sector and Narrow-Beam Trisector Cell (NBTC) types are mentioned by [7].

Table 6.1: The Three Directional Antennas

Antenna Pattern	Source Cited
Wide-Beam Trisector Cell with Diamond-Shaped Sector	[7]
Narrow-Beam Trisector Cell	[7]
Wide-Beam Trisector Cell with Pentagon-Shaped Sector	[5]

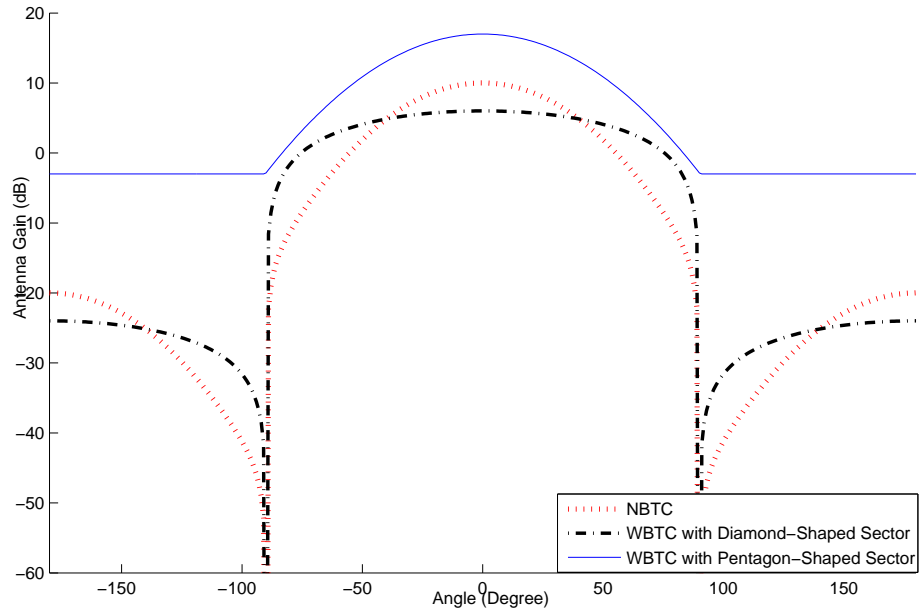


Figure 6.1: Antenna Gain

The gains of the three directional antenna patterns are shown Fig. 6.1. The main-lobe is located in 0° and the gain angle is ranging in -180° to 180° . There is some small amount of leakage in the side-lobe. The front-to-end power ratio is constant in the WBTC with Pentagon-Shaped Sector pattern.

In the multi-cell environment, we use “BS-to-BS distance” instead of “cell coverage” in this thesis since the cell architectures are not circular. For comparison, the BS-to-BS distance among the three systems will be the same. So the density of BS is the same. In Fig. 6.2 we can see the adjacent cells multi-cell environment under the same BS density.

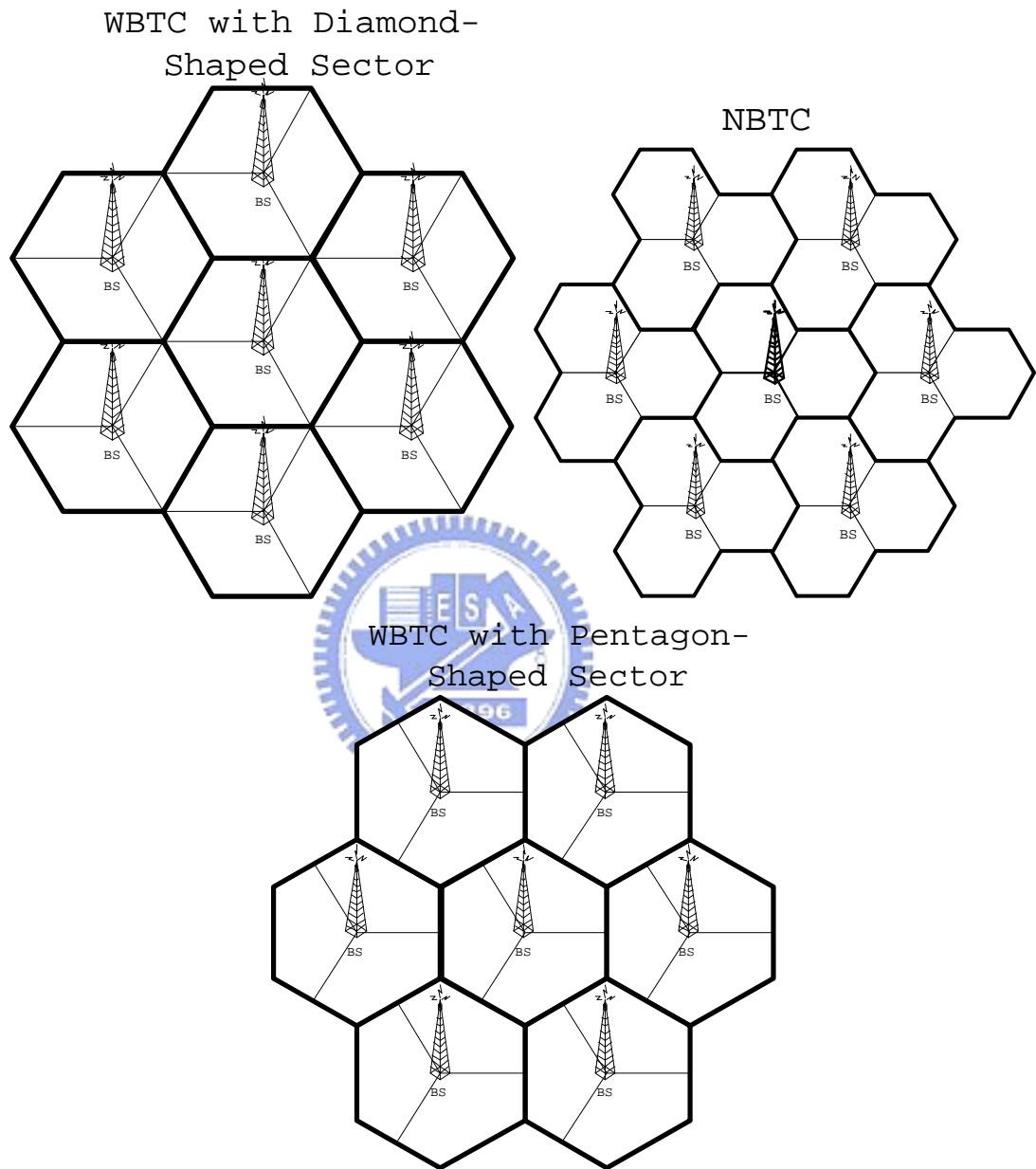


Figure 6.2: The Three Antenna Patterns in Multi-Cellular Environment

WBTC with Diamond-Shaped Sector

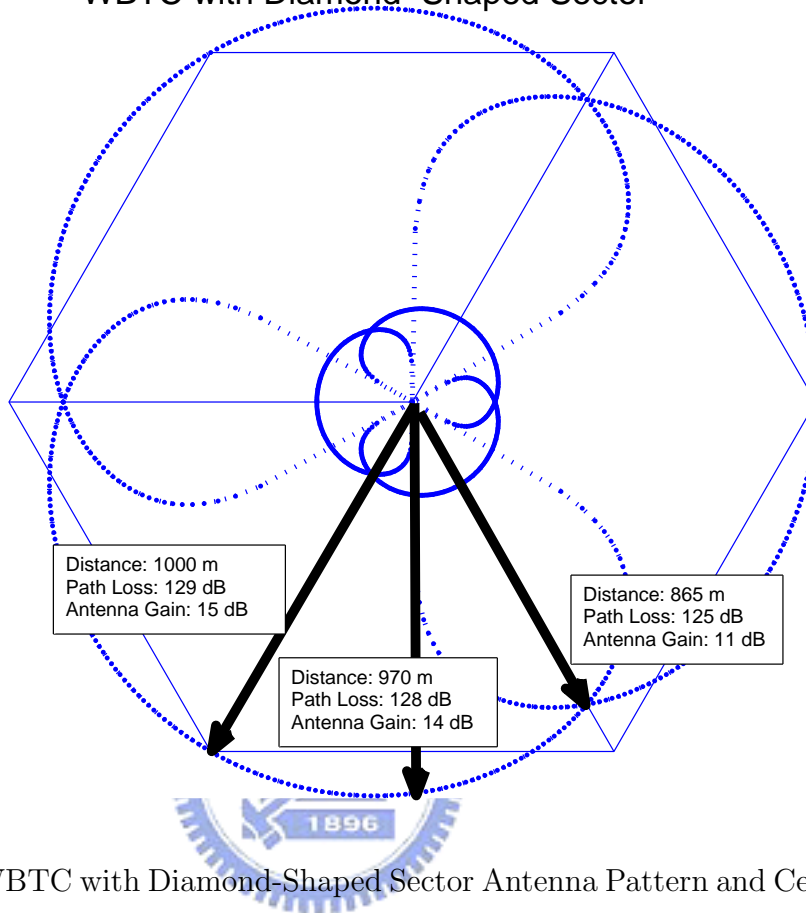


Figure 6.3: WBTC with Diamond-Shaped Sector Antenna Pattern and Cell Boundary

6.1.1 WBTC with Diamond-Shaped Sector

WBTC with Diamond-Shaped Sector antenna uses a 120° antenna pattern in each sector. The shapes of the sectors are diamonds and form the cell structure as a hexagon. It's most conventional for multi-cellular systems.

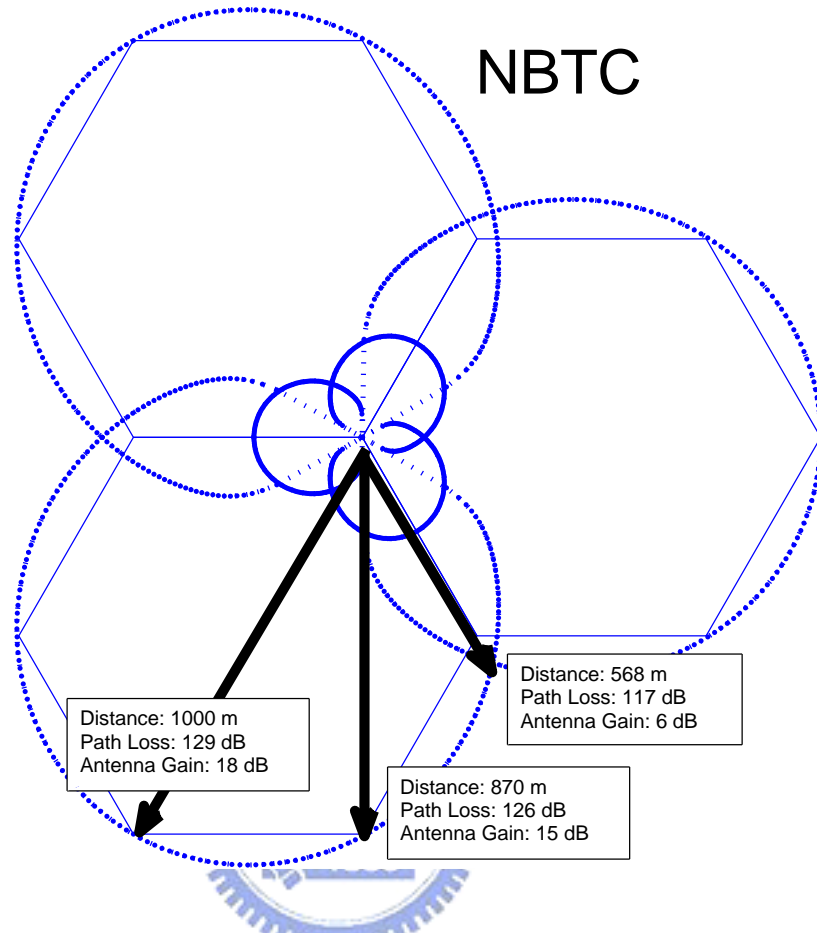


Figure 6.4: NBTC Antenna Pattern and Cell Boundary

6.1.2 NBTC

NBTC uses a 60° antenna in each sector. The shape of the sector is a hexagon. Three antennas form the cell structure as a clover leaf. The energy leakage in the side-lobe is smaller than WBTC type.

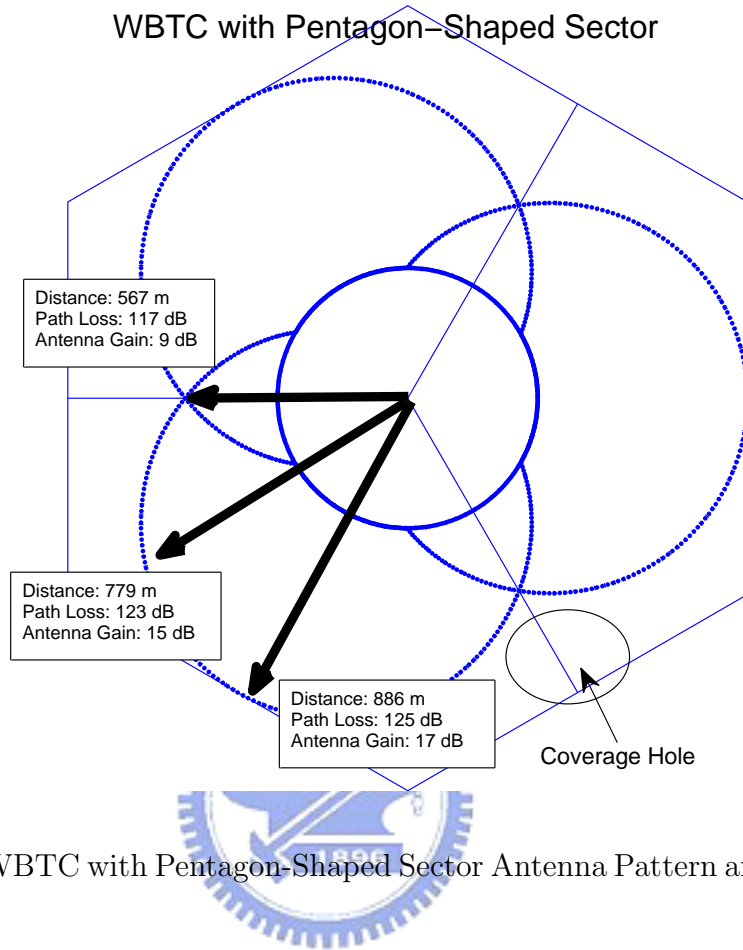


Figure 6.5: WBTC with Pentagon-Shaped Sector Antenna Pattern and Cell Boundary

6.1.3 WBTC with Pentagon-Shaped Sector

WBTC with Pentagon-Shaped Sector antenna pattern uses an 120° antenna pattern as that in WBTC with Diamond-Shaped Sector antenna pattern. There is 30° -angle rotation between them. The antenna pattern is specified as (6.1). As shown in Fig. 6.1, the coverage hole in the cell boundary is larger than the other two antenna types.

$$A(\theta) = -\min\left[12\left(\frac{\theta}{\theta_{3dB}}\right)^2, A_m\right] \quad (6.1)$$

where $A(\theta)$ is the antenna gain, θ_{3dB} is the 3 dB beam-width. The default θ_{3dB} is 70° . $A_m = 20$ dB is the maximum attenuation.

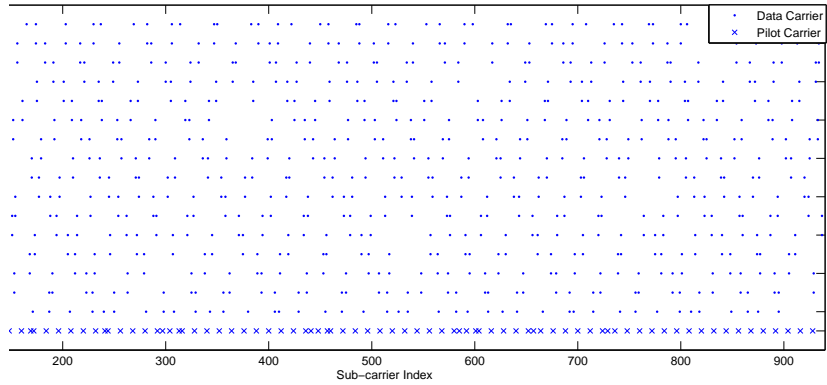


Figure 6.6: The Sub-Channels and Pilots in FUSC Permutation

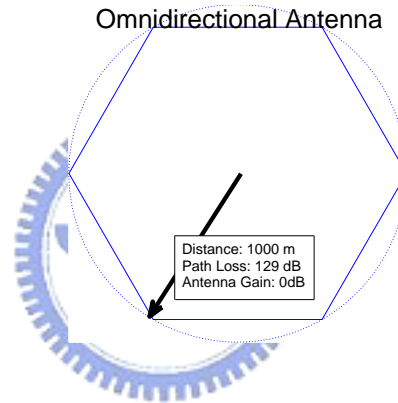


Figure 6.7: Omnidirectional Antenna Pattern and Cell Boundary

6.2 Omnidirectional Antenna and FUSC

For comparison, we also consider the omnidirectional antenna in this system. The antenna gain in omnidirectional antenna system is assumed 0 dB in each direction. The sub-carriers in FUSC spread in the whole band, so FUSC is suitable in omnidirectional antenna application and broadcast purpose. Fig. 6.6 shows the locations of the 16 sub-channels and pilots in FUSC permutation. The cell structure is a hexagon and the antenna pattern is a round shape in Fig 6.7.

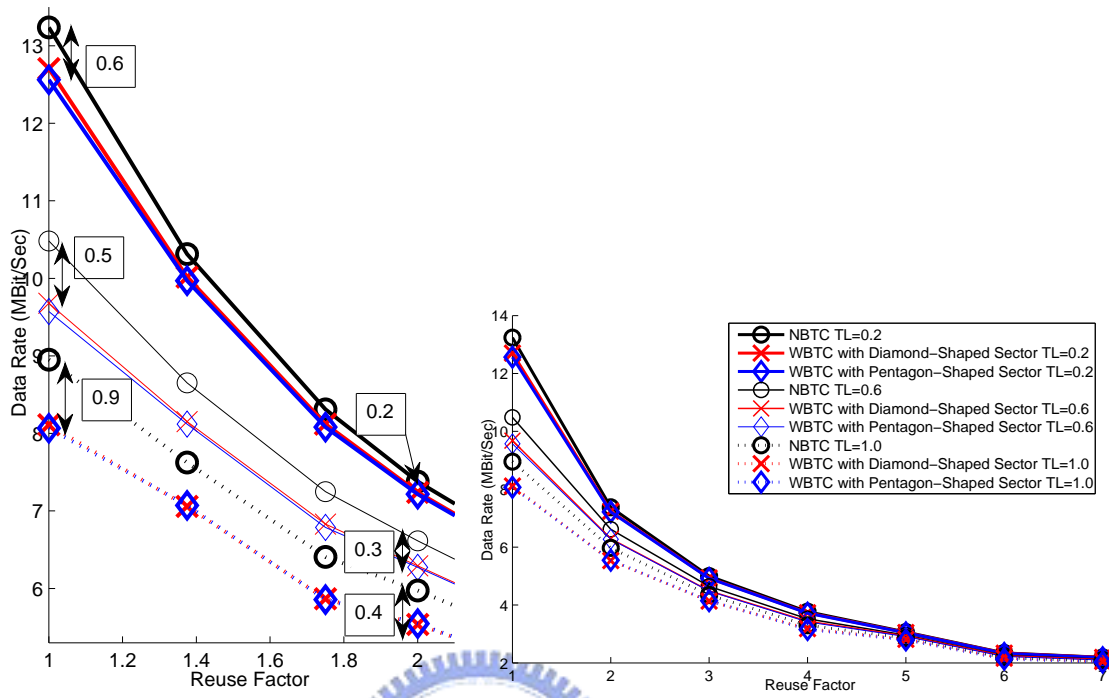


Figure 6.8: Cell Capacity in Three Different Directional Antennas

6.3 Numerical Results

6.3.1 Effect on Throughput

The system capacity will decrease as reuse factor N increases. The NBTC type is the best type in terms of throughput as shown in Fig. 6.8. The NBTC gets more 0.2 to 0.9 Mbps throughput when reuse factor is about 1 or 2. The capacity of WBTC with Diamond-Shaped Sector and WBTC with Pentagon-Shaped are similar. This is because the cell structures of WBTC with Diamond-Shaped Sector and WBTC with Pentagon-Shaped Sector are similar. Both of them are hexagon structure.

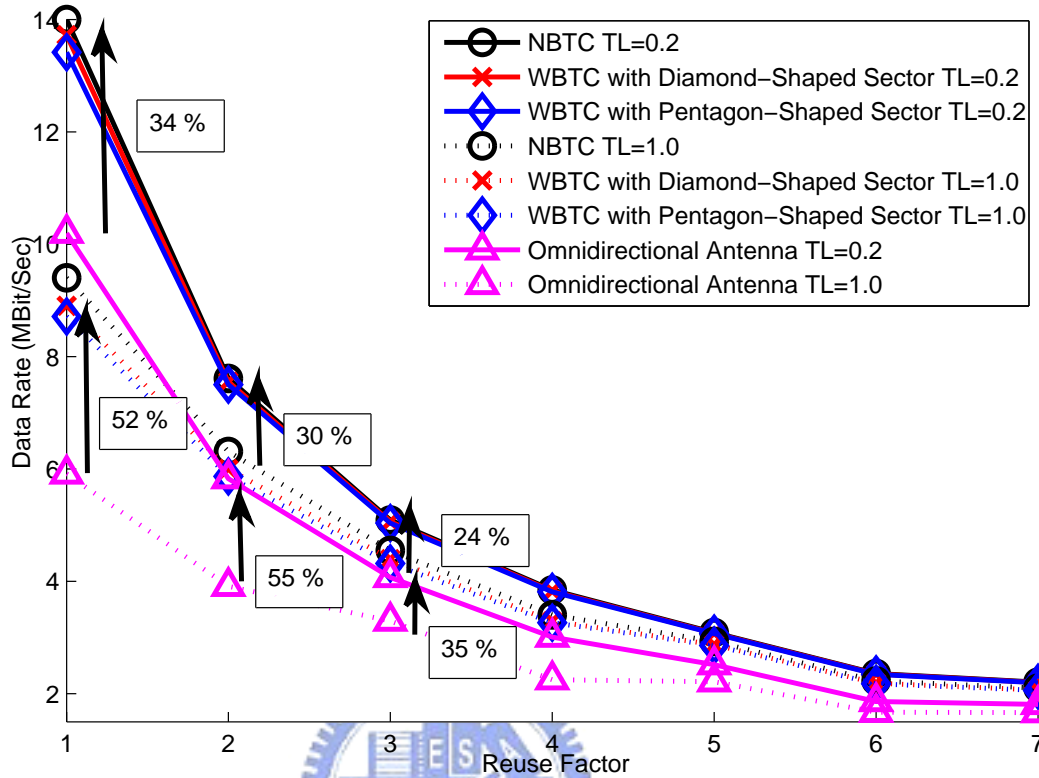


Figure 6.9: Cell Capacity in Directional and Omnidirectional Antennas

The gain between directional and omnidirectional antenna patterns are larger. In Fig. 6.9, the cells with the directional antennas get more 24% to 55% capacity than omnidirectional antenna systems. In high traffic load, the improvements are larger.

6.3.2 Effect on Link Quality

The 90% tile of users' received SINR is shown in Fig. 6.10. The omnidirectional antenna system gets less 9.6 to 13.8 dB link quality than the directional antenna systems. This is because the co-channel interference in omnidirectional systems is higher

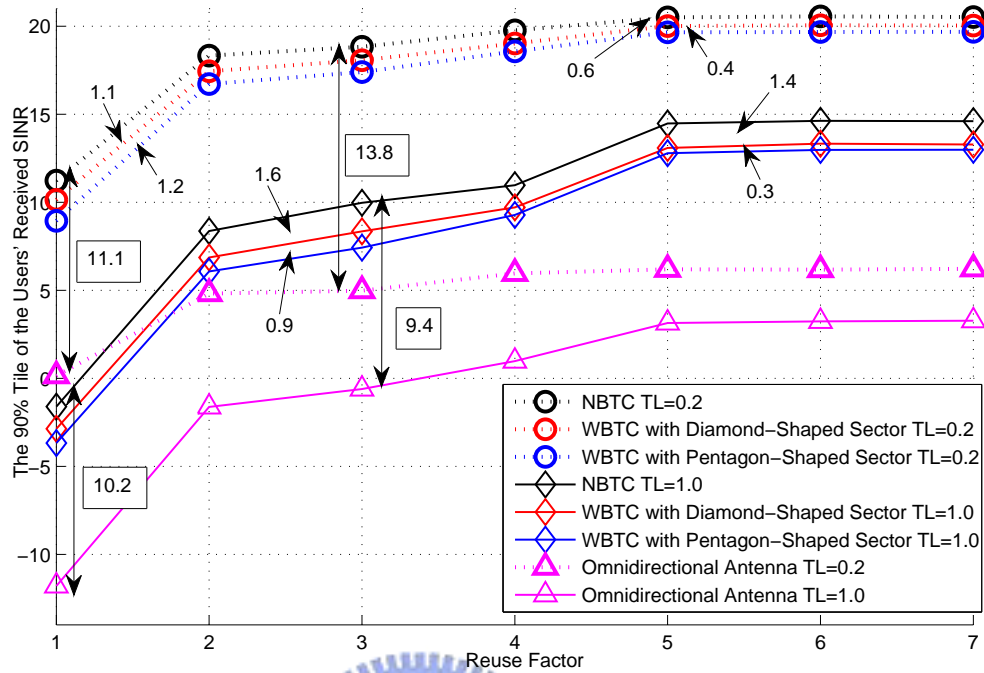


Figure 6.10: The 90% tile of Users' Received SINR in Different Antennas

than that in directional antenna systems. The link quality of the NBTC antenna pattern is the best. The WBTC with Pentagon-Shaped gets the worst performance in the three directional antennas. The NBTC can get more 0.6 to 1.4 dB link quality than the other two directional antenna. The largest improvement of the link quality is in the range when reuse factor is about one or two.

6.3.3 Effect on the Capacity and Fairness of Inner/Outer Users

Fig. 6.11 and 6.12 show the capacity in the inner and outer users. For inner users, the differences of these three types are not obvious, especially for $RF > 1$. This is because the inner users get larger signal strength, so the SINR of them changes little

when antenna pattern changes.

For outer users, there are larger improvements in NBTC type. In high interference traffic load, there are good improvements when reuse factor is about two. Outer users' capacity can be boosted by 15 % to 24 %. The improvements are larger in WBTC with Diamond-Shaped Sector and WBTC with Pentagon-Shaped types. Because of the better performance of outer users, NBTC is the fairest type of the three types.

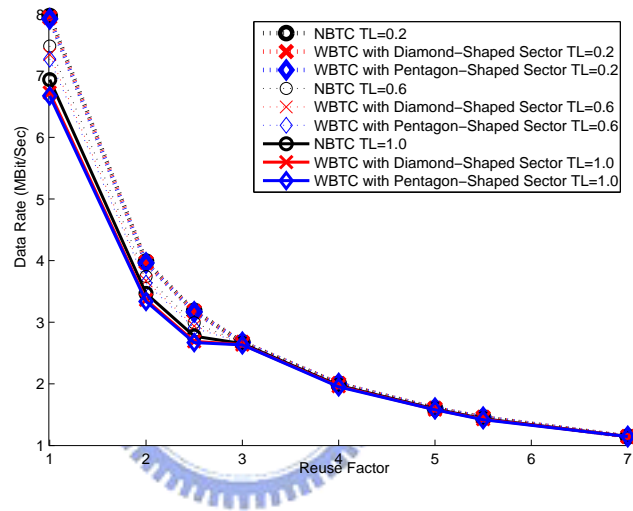


Figure 6.11: Inner Users' Throughput in Three Different Directional Antennas

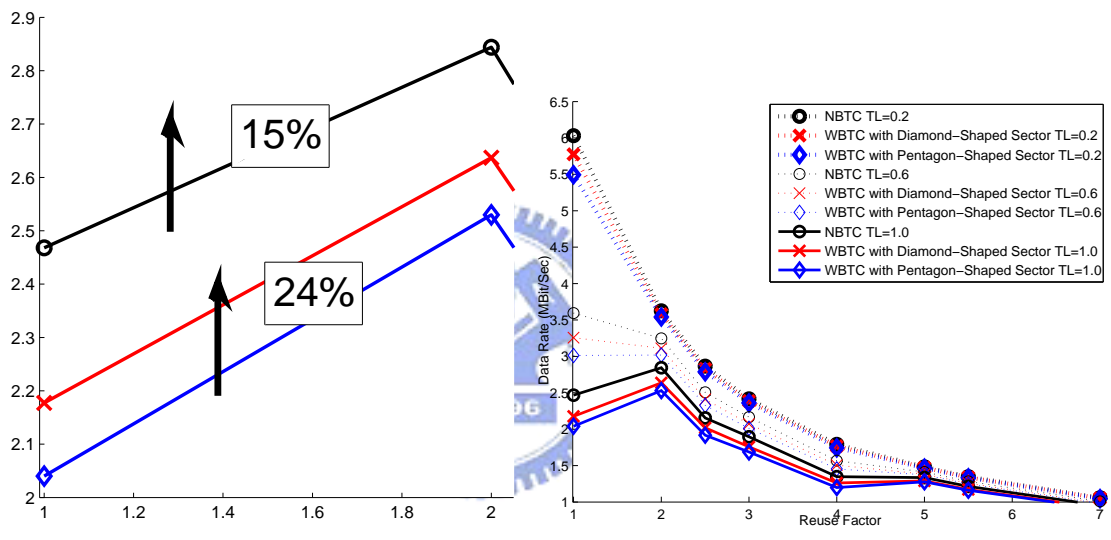


Figure 6.12: Outer Users' Throughput in Three Different Directional Antennas

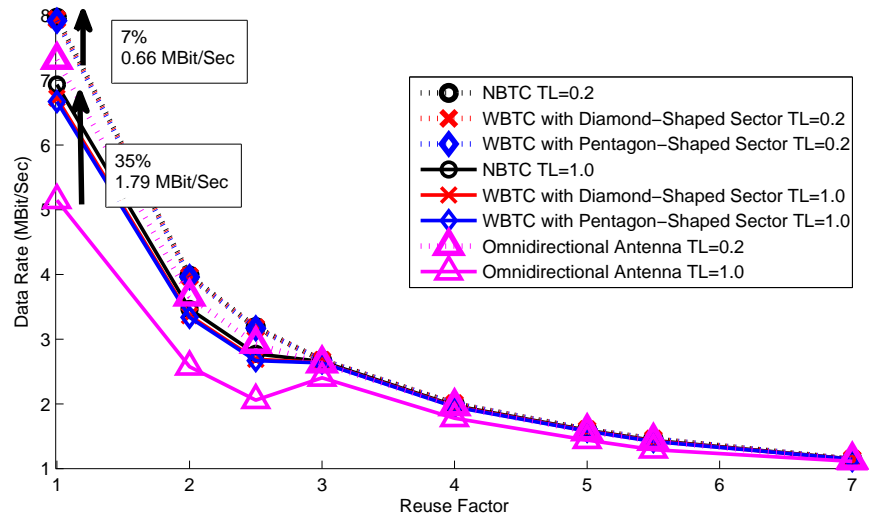


Figure 6.13: Inner Users' Throughput in Directional and Omnidirectional Antennas

The usage of directional antenna gives lots of help for the outer users. In Fig. 6.13 and 6.14, we can see the inner/outer users get more throughput than in omnidirectional antenna systems. The outer users get more merits from directional antennas.

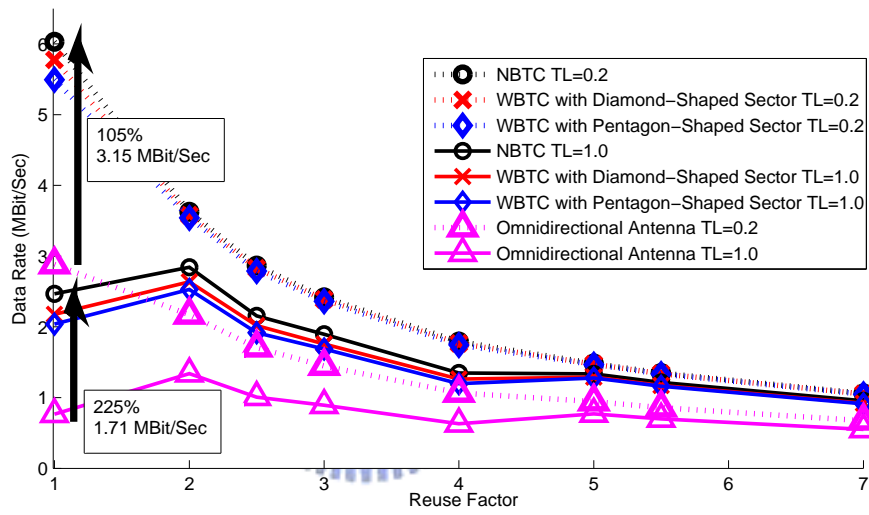


Figure 6.14: Outer Users' Throughput in Directional and Omnidirectional Antennas

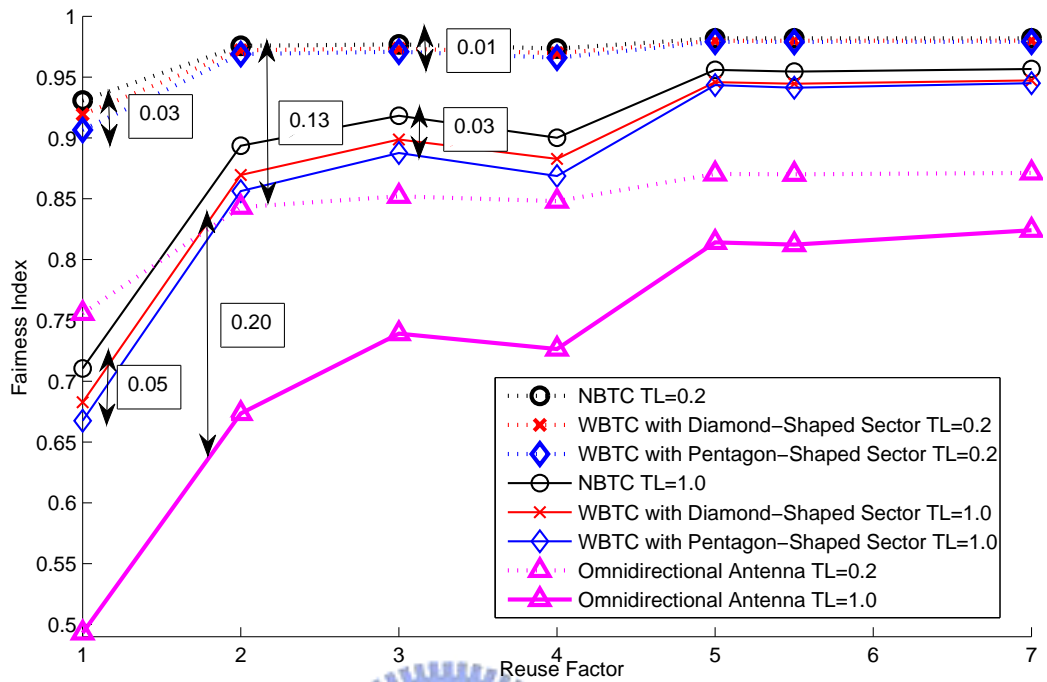


Figure 6.15: The Fairness of the Users in Directional and Omnidirectional Antenna Systems

In the fairness issue, the best antenna type is the NBTC antenna pattern. The fairness of the NBTC systems gets more 0.01 to 0.05 than the other two directional antennas. Compared to the omnidirectional systems, directional antenna system gets more 0.13 to 0.20 in fairness index.

CHAPTER 7

Conclusion and Future Work

7.1 Conclusion

We get some important quantitative analysis results in the OFDMA multi-cellular system. The performance of the PHY layer with IEEE 802.16 WiMAX specification is preliminary discussed. This thesis can give the network provider some important information before they deploy the IEEE 802.16 WiMAX network. These quantitative analysis results also help the researchers. Researchers may estimate the performance of the network and when they want to verify their theoretical algorithms.

7.1.1 Permutation

The randomization of sub-carriers helps in link quality. The distributed type permutation can earn more 7.4 to 8.0 dB SINR for the 90 % tile users. The interference is eased by the randomized permutation. In PUSC Type 1, the co-channel interference from the adjacent cells is randomized. The SINR performance of PUSC Type 1 is better than PUSC Type 0. Even combined with frequency reuse, we find that the PUSC Type 1 is also better than the PUSC Type 0. This is because the interference

strength is weakened by the larger interference source path loss. PUSC Type 0 needs additional cooperating efforts among BSs and we can save the efforts.

The distributed permutation also gets some merits in frequency selective fading channel. Band AMC is not suitable in the frequency selective fading channel model because of the deep fading of the channel.

7.1.2 Regular/Fractional Frequency Reuse

The frequency reuse can improve the capacity of the outer users. The fairness will improve when we use the frequency reuse, too. The outer users may get more 7% to 40% capacity. In this thesis, the case $N=2$ is a suggested reuse factor for the fairness. Since higher N we get limited improvement of fairness but throughput of the outer and total users shrinks in large N .

However, with fractional frequency reuse, the capacity of the system will decrease as reuse factor increasing. Even through frequency reuse can reduce the co-channel interference and users can get higher SINR, the capacity will shrink due to the reduce of the usable frequency band.

7.1.3 Directional Antenna

We suggest that the NBTC antenna type is better in the multi-cell systems. The system can get more 24% to 55% Mbps in total throughput when we use directional antenna pattern. The performance of NBTC is the best. WBTC with Diamond-Shaped Sector and WBTC with Pentagon-Shaped Sector antenna types are similar. This gives the network provider a better choice when spreading the BSs.

7.2 Future Work

7.2.1 Benefit of Band AMC

There may be some methods to improve the performance of Band AMC. If the channel is flat fading and varies with time slowly, the performance of Band AMC may be better with some scheduling. The sub-carrier of PUSC is distributed in the whole frequency band so the difference of the sub-channels' channel gains in PUSC will not be very large. The Band AMC may take advantage from water-filling because of the differences of the Band AMC sub-channels are larger.

Another property of Band AMC is the scalable time duration of a Band AMC symbol. A Band AMC symbol may occupy 1, 2, 3, or 6 OFDMA symbols in time domain. Maybe some adaptive scheduling method can take advantage of this property in the time varying channel. For example, if a symbol time is 1 ms, and coherence time is 8 ms, we can use Band AMC sub-channel with 6 OFDMA symbols in time domain (Type 4).

7.2.2 Proportional Fair Scheduling

Proportional fair scheduling is suggested in IEEE 802.16m evaluation methodology [5]. In this thesis we use the round robin method. Proportional fair scheduling concerns about the throughput and the delay of the user. It's helpful in fairness and latency of the network.

In [16], the priority function P of the i_{th} station under proportional fair scheduling can be (7.1). BS can control users' sub-channel resource based on priority function

P_i .

$$P_i = \frac{T_i^\alpha}{R_i^\beta} \quad (7.1)$$

where T_i is the data rate of the i_{th} station this time slot; R_i is the data rate of the i_{th} station during some period of time; α and β are tunable for the fairness.



Bibliography

- [1] Mugdim Bublin, et al., "Interference Averaging Concepts", *PIMRC*, Athens, Sep 2007
- [2] Geneieve Mange, et al., "Interference Avoidance Concepts", *PIMRC*, Athens, Sep 2007
- [3] Magnus Olsson, et al., "Smart Antenna Based Interference Mitigation", *PIMRC*, Athens, Sep 2007
- [4] Leonard J. Cimini, JR., et al., "Analysis and Simulation of a Digital Mobile Channel Using Orthogonal Frequency Division Multiplexing", *IEEE Trans. ON Communi.*, Jul 1985
- [5] Intel, Motorola, Beceem, Nortel, Samsung, Draft IEEE 802.16m Evaluation Methodology", *IEEE 802.16 Broadband Wireless Access Working Group*, Oct 2007
- [6] V. Erceg, K. V. S. Hari, M. S. Smith, D. S. Baum, et al., Channel Model for Fixed Wireless Applications", *IEEE 802.16 Broadband Wireless Access Working Group*, Aril 2001
- [7] Li-Chun Wang, A new cellular architecture based on an interleaved cluster concept", *IEEE Transactions on Vehicular Technology*, Nov 1999
- [8] C.F. Ball, E. Humburg, K. Ivanov, F. Treml, Siemens AG, Performance Analysis of IEEE802.16 Based Cellular MAN with OFDM-256 in Mobile Scenarios", *IEEE Transactions on Vehicular Technology*, Nov 2005
- [9] Gamini Senarath, et al., Multi-hop Relay System Evaluation Methodology, *IEEE 802.16 Broadband Wireless Access Working Group*, Oct 2006
- [10] Aditya Agrawal, et al., Air Interface for Fixed and Mobile Broadband Wireless Access Systems: IEEE Std 802.16e, *IEEE Computer Society and the IEEE Microwave Theory and Techniques Society*, Feb 2006
- [11] V.H. Mac Donald, The Cellular Concept, *The Bell System Technical Journal*, Jan 1979
- [12] WiMax Forum, Mobile WiMAX-Part I: a Technical Overview and Performance Evaluation, *WiMax Forum*, Aug 2006
- [13] I-Kang Fu, Hsiang-Jung Chiu and Wern-Ho Sheen, An Improved Fast Base Station Switching for IEEE 802.16e with Reuse Partitioning, *NCTU*, 2007

- [14] R. Jain, G Babic, B. Nagendra, and C. Lam, Fairness, call establishment latency and other-performance metrics, *The University of Texas at Austin, AT&T Lab Inc.*, Feb 2007
- [15] Jeffrey G. Andrews, Arunabha Ghosh, Rias Muhamed, Fundamentals of WiMAX Understanding Broadband Wireless Networking, *Tech. Rep ATM Forum/96-1173, ATM Forum Document*, Aug 1996
- [16] Yang, Ji, Average Rate Updating Mechanism in Proportional Fair Scheduler for HDR, *IEEE Global Telecommuni. Conf.*, 2004



Vita

Wei-Hsien Huang

He was born in 1978. He received a B.S. in Electronic and Control Engineering from National Chiao-Tung University in 2001. From July 2005 to July 2008, he worked his Master degree in the Wireless System Lab in the Department of Communication Engineering at National Chiao-Tung University. His research interests are in the field of wireless communications.

